THESIS

DIVERSE DEVELOPMENTAL TRAJECTORIES OF PERINEURONAL NETS DURING VERTEBRATE NERVOUS SYSTEM CONSTRUCTION

Submitted by

Jacob Edwards

Department of Biology

In partial fulfillment of the requirements

For the Degree of Master of Science

Colorado State University

Fort Collins, Colorado

Spring 2018

Master's Committee:

Advisor: Kim Hoke

Charles Anderson
Deborah Garrity
Rachel Mueller

ABSTRACT

DIVERSE DEVELOPMENTAL TRAJECTORIES OF PERINEURONAL NETS DURING VERTEBRATE NERVOUS SYSTEM CONSTRUCTION

In the central nervous system, aggregated extracellular matrix compounds known as perineuronal nets (PNNs) shape patterns of neural connectivity over development. Removing PNNs restores juvenile-like states of neural circuit plasticity and subsequent behavioral plasticity. Our current understanding of the role of PNNs in plasticity has resulted in promising therapeutic applications for many neurodegenerative diseases. To ensure safety and efficacy in such applications, we require a broad understanding of PNN function in the nervous system. The current data suggest that PNNs stabilize fundamental features of neural connectivity progressively in an ascending, or "ground-up", fashion. Stabilizing lower input processing pathways establishes a solid, reliable foundation for higher cognition. However, data on PNN development exists almost exclusively for mammals. Is, then, the ground-up model of circuit stabilization a general feature of PNNs across vertebrates? I found that developmental patterns of PNNs in fish (*Poecilia reticulata*), amphibians (*Rhinella yunga*), and reptiles (*Anolis sagrei*) follow diverse trajectories, often emerging first in higher forebrain processing pathways. Similarly, they associate with diverse cell populations and vary widely in structural characteristics both within and across species. While my data do not invalidate a ground-up model for mammal PNNs, they do suggest that this pattern may be an evolutionary innovation in this group, and that the broad roles of PNNs in circuit stability and neuronal physiology are complex and lineage-specific.

ACKNOWLEDGEMENTS

First and foremost, I thank my gracious advisor, Kim Hoke, for her endless patience, encouragement, and constructive feedback throughout my two-and-a-half-year tenure as a graduate student in Fort Collins. Kim, I found very early on that you have a unique ability to detect what projects and experiments would suit my fascination before I could ever have managed to articulate them. Your mentoring and scientific philosophies have made an enduring mark on me. Thank you!

Second, I thank the incredible graduate student community at CSU for being my rock throughout incredibly fun times as well as hardships. Coffee breaks, happy hours, gorgeous hikes, and spending too many nights on the town too late into the evening are some of my fondest memories of Colorado. There are too many of you to thank to list by name. It was the greatest pleasure to be your colleague and I can't wait to catch up when our paths cross again.

Third, I thank my generous committee, Chuck Anderson, Debbie Garrity, and Rachel Mueller for your excitement and encouragement regarding my project and intellectual interests. You certainly helped me push my own boundaries, each in your own way.

Fourth, I thank the numerous academics at CSU and beyond who believed in my passion and spent their valuable time shooting wild intellectual discussions with me: Colleen Webb, Carol Seger, Dan Sloan, Reddy, Yoko Yazaki-Sugiyama, Sarah Woolley, Jon Prather, Dan Medeiros, Marc Schmidt, Larry Abbott, and others. While most of them will never see this document, their time and willingness to discuss lofty ideas made a lasting impression on me. Of course, I must thank the excellent Hoke-Funk labs for creating a healthy, fun work environment, in particular: Kim Dolphin, Laura Stein, Leorah McGinnis, Molly Womack, Jenny Stynoski, and

Eva Fischer. Finally, to my two stalwart undergraduates: Justine Stalnaker and Makayla Risch. What a pleasure it was to see you take on your own projects and it was my greatest honor to be your mentor and witness the growth of your curiosity and discoveries. Keep exploring!

Last, I thank my family back home in Tennessee: Mom, Dad, Jonny, and Sam, for always having my back no matter what. Knowing you were there rooting for me the whole time got me through some of the hardest struggles of an endeavor like this.

TABLE OF CONTENTS

LIST OF TABLES

LIST OF FIGURES

CHAPTER 1: OVERVIEW

Neural networks that drive animal behavior develop under the guidance of an inherited genetic program, yet are simultaneously susceptible to rewiring following sensory experience or learning. Decades of research have identified mechanisms that explain the balance of neural connection updating (*plasticity*) with maintenance, or homeostasis (*stability*), from long-term potentiation and depression at the synapse level (Malenka & Bear 2004), modification of ion channel parameters at the cellular level (O'Leary *et al.* 2013), to synaptic scaling that results in stability across circuits (Turrigiano 2008). Such a dynamic interplay of stabilizing and destabilizing forces points to an intricate balance of neural plasticity and stability in the central nervous system (CNS), achieved by cells and the types of input they receive (Schulz 2006).

Mechanisms that permit plasticity, such as strengthening or weakening of synaptic partnership due to spike-timing-dependent activity, drive neural systems into patterns of excitation or inhibition that adapt an individual to its environmental demands. But models including plastic changes alone demonstrate that systems tend toward extremes, with a result of over-excitation or -inhibition to stimuli, leading to irresolvable overload by the time signals reach higher processing areas, or complete loss of signal transduction (Abbott & Nelson 2000; Mermillod 2013). So-called "homeostatic" mechanisms enter to stabilize and tune neural systems such that plasticity is possible along with maintenance of signal integrity (Turrigiano 2008).

While much of our understanding of the balance of plasticity and stability in the CNS rests on the behavior of neurons and their supportive glial cells, recent years have seen the neural extracellular matrix (ECM) as a key player in maintaining plasticity/stability balance over developmental time (Celio *et al.* 1998; Takesian & Hensch 2013; Miyata & Kitagawa 2017).

Highly structured, lattice-like ECM compounds envelop specific neuronal subtypes in specific brain regions during development. Cells expressing the membrane-bound protein hyaluronan synthase secrete a hyaluronic acid chain into the extracellular space, which binds chondroitin sulfate proteoglycans, link proteins, and tenascins to create a web of coating around neurons, known as the perineuronal net (PNN; Kwok *et al.* 2011). Work in mammalian visual, somatosensory, and auditory systems has identified that PNNs preferentially surround the soma and proximal dendrites of large, fast-spiking, inhibitory, parvalbumin-positive (PV+) interneurons upon exposure to orthodenticle homeobox 2 protein (Otx2) synaptically transmitted from sensory input cells, such as retinal ganglion or whisker cells (Friauf 2000; Hensch 2005; McRae *et al.* 2007; Sugiyama *et al.* 2008). Thus, PNN development is dependent on signal transduction between neurons. PNNs further protect their neurons from firing-induced oxidative stress, provide an ionic buffering environment, and enhance excitability. In sum, they enable rapid and prolonged bursting behavior that has strong influence on participating neural circuits (Härtig *et al.* 1999; Cabungcal *et al.* 2013; Hu *et al.* 2014; Balmer 2016).

Critically, however, PNNs act as a physical and chemical blockade for approaching axonal growth cones, thereby ending developmental periods of activity-dependent rewiring. PNNs are impenetrable physical structures for growth cones, harbor repulsive molecules such as semaphorins, and spatially corral neurotransmitter receptors (Sorg *et al.* 2016). By and large, then, the emergence of PNNs in a given brain region has been taken as a sign of a "mature" circuit component, one that is no longer capable of establishing new synaptic partners regardless of the strength, frequency, or source of input (see *e.g.* Köppe *et al.* 1997).

An ever-growing body of literature spanning multiple animal species, brain regions, and behavioral assays supports the role of circuit stabilization by PNNs. The end result of most

empirical studies removing PNNs in adulthood is a return of functional neural and behavioral plasticity. In 2002, Pizzorusso *et al.* were the first to demonstrate that degrading PNNs with the enzyme chondroitinase ABC (ChABC) restored ocular dominance plasticity to visual circuits in adult rats, a feat typically possible only during a critical period of development that ends in the third week of life. Since then, numerous experiments have reported a ChABC-induced return of critical period-like plasticity and learning capacity in adult animals and in a variety of behaviors, including fear memory extinction (Gogolla *et al.* 2009), fear learning (Hylin *et al.* 2013), object recognition memory (Romberg *et al.* 2013), auditory tone reversal learning (Happel *et al.* 2014), and motor recovery from spinal cord injury (Wang *et al.* 2011).

These studies among others have inspired promise of PNN manipulation for improving human learning capacity, therapy for addiction, and CNS damage. However, because they have almost exclusively been studied in mammals, it has been largely ignored that PNNs may be a fundamental feature of vertebrate biology and a critical regulator of CNS plasticity over development. While PNNs are found broadly throughout the mammalian CNS (Figure 1.1), Brückner *et al.* (1994; 1998) and Mueller *et al.* (2016) have been among the few to observe and consider species and sex differences in PNN expression, finding stark differences between even closely related rodent species both within and between brain regions (Brückner *et al.* 1994), and between rodents and primates (Mueller *et al.* 2016), possibly representing differences in environmental and behavioral demands for plasticity. Along this line, one study reported that PNNs in the avian (zebra finch; *Taenioypygia guttata*) song-learning and song-production system emerge likewise in an experience-dependent and developmentally regulated fashion (Balmer *et al.* 2009). While preliminary experiments with ChABC PNN removal failed to restore the song-learning critical period in this species, further observations by Cornez *et al.* (2017)

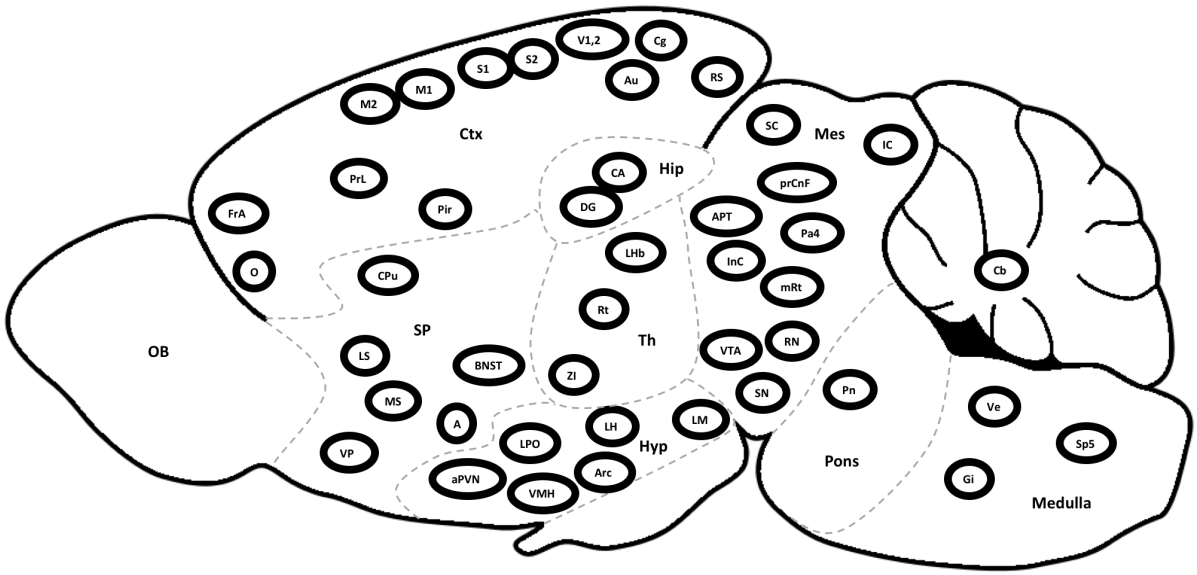

Figure 1.1. Distributions of PNNs in mouse, *Mus musculus*. Black circles indicate regions containing PNNs. Based on [1]Horii-Hayashi *et al.* (2015), [2]Brückner *et al.* (2000). Sagittal view with PNN-containing regions positioned roughly into major brain divisions, collapsed along medial-lateral axis, using Allen Brain Atlas (2008). Anterior/rostral regions leftmost, posterior/caudal regions rightmost. OB, olfactory bulb; Ctx, cortex; SP, subpallium; Hip, hippocampus; Th, thalamus; Hyp, hypothalamus; Mes, mesencephalon; Cb, cerebellum. See Table 1.1 for list of abbreviations.

demonstrated that PNNs are present, though significantly less dense, in songbird species capable of seasonal song updating versus those that pass through a critical period for song-learning (such as zebra finches). Further supporting the concept that PNNs may contribute directly to the plasticity of learned, ecologically relevant behaviors was the finding that PNNs are also greatly reduced in female zebra finches, who do not learn to sing or produce song-like vocalizations (Meyer *et al.* 2014; Cornez *et al.* 2015). In sum, there remains immense potential to explore the evolution of animal neural and behavioral development by considering how the neural ECM, particularly PNNs, contribute to the balance of plasticity and stability in the vertebrate CNS.

Table 1.1. List of abbreviations used in figures and text for brain regions across taxa. Mammalian abbreviations from Horii-Hayashi *et al.* (2015), others from Nieuwenhuys *et al.* (1998).

Mammals

A	Amygdala	LH	Lateral hypothalamus	Rt	Reticular thalamic nucleus
APT	Anterior pretectal nucleus	LM	Lateral mammillary nucleus	S1	Primary somatosensory cortex
aPVN	Anterior paraventricular nucleus	LPO	Lateral preoptic area	S2	Secondary somatosensory cortex
Arc	Arcuate nucleus	LS	Lateral septum	SC	Superior colliculus
Au	Primary auditory cortex	M1	Primary motor cortex	SN	Substantia nigra
BNST	Bed nucleus of the stria terminalis	M2	Secondary motor cortex	Sp5	Spinal trigeminal nucleus
CA	Hippocampus, CA1-3	mRt	Mesencephalic reticular formation	V1	Primary visual cortex
Cb	Cerebellum	MS	Medial septum	V2	Secondary visual cortex
Cg	Anterior cingulate	O	Orbital cortex	Ve	Vestibular nuclei
Cpu	Caudate putamen	Pa4	Paratrochlear nucleus	VMH	Ventromedial hypothalamic nucleus
DG	Hippocampus, dentate gyrus	Pir	Piriform cortex	VP	Ventral pallidum
FrA	Frontal association cortex	Pn	Pontine reticular nuclei	VTA	Ventral tegmental area
Gi	Gigantocellular reticular nucleus	prCnF	Precuneiform area	ZI	Zona incerta
IC	Inferior colliculus	PrL	Prelimbic cortex		
InC	Interstitial nucleus of Cajal	RN	Red nucleus		
LHb	Lateral habenular nucleus	RS	Retrosplenial cortex		

Fish

CH	Caudal hypothalamus	DH	Dorsal hypothalamus	rets	Medullar reticular nuclei
CG	Central (periaqueductal) grey	nMLF	Nucleus of the MLF	MLF	Medial longitudinal fascicle

Frogs

A	Amygdala	MP	Medial pallium	TP	Posterior tuberculum
DH	Dorsal hypothalamus	Pr	Principal nucleus of the torus semicircularis	VL	Ventrolateral thalamic nucleus
Iflm	Interstitial nucleus of the MLF	rets	Medullar reticular nuclei	MLF	Medial longitudinal fascicle
LP	Lateral pallium	SC	Suprachiasmatic nucleus		

Reptiles

Alh	Lateral hypothalamic area	Lte	Lentiform nucleus of the thalamus	Sel	Lateral septum
Cb	Cerebellum	Pb	Parabrachial nucleus	sgc	Stratum griseum centrale (optic tectum)
CMN	Cranial motor nuclei	Rai	Inferior raphe nucleus	SO	Supraoptic nucleus
Iflm	Interstitial nucleus of MLF	Ri	Inferior reticular nuclei	Vest	Vestibular nuclei
Inst	Bed nucleus of the stria terminalis	Rm	Medial reticular nuclei	VI	Nucleus of the abducens nerve
LC	Locus coeruleus	Rs	Superior reticular nuclei	Vlt	Ventrolateral thalamic nucleus
Ll	Lateral lemniscus	SC	Subcoeruleus area	VTA	Ventral tegmental area

The emerging model of PNNs over CNS development is that they stabilize fundamental neural connections in the developing animal in a ground-up fashion. Lower sensory input connectivity is established and maintained by PNNs, which provides a reliable source of input for higher processing areas (Takesian & Hensch 2013). However, whether this is a feature of vertebrate CNS development in general, or simply an observation from studying mammals has yet been challenged. In this thesis, I test two major hypotheses regarding the broad roles of PNNs across vertebrates: **(1)** PNNs envelop the same brain regions and cell types (putative fast-firing PV neurons) across species, and **(2)** stepwise circuit stabilization across development is a conserved feature of PNN expression. I characterize the spatial, structural, and temporal emergence of PNNs, and their PV-cell associations, across the CNS of fish, amphibians, and reptiles; three major vertebrate clades which have received little to no attention in the neural ECM literature. I found **(1)** that PNNs envelop neurons in a wide range of brain regions, take on diverse architectures, and variably associate with putative fast-firing PV-positive neurons. I then map the developmental trajectories of PNNs across development of each species, showing **(2)** that PNN development is region- and lineage-specific, and that the vertebrates studied here develop PNNs in a fashion contrasting the model inspired by mammalian research. I found that PNNs, in contrast to the ground-up model, emerge first in fore- and mid-brain regions responsible for modulating behavioral states, and only later develop in lower processing regions that route incoming sensory and outgoing motor signals.

CHAPTER 2: SPATIAL, STRUCTURAL DIVERSITY, AND CELLULAR ASSOCIATIONS OF PERINEURONAL NETS

Introduction

Perineuronal nets (PNNs) are structured extracellular matrix (ECM) compounds that envelop neurons during postnatal development (Celio *et al.* 1998; Hensch 2005; Miyata & Kitagawa 2017). They are composed of a hyaluronan backbone tethered to chondroitin-sulfate proteoglycans, and are found throughout the central nervous system (CNS) of mammals (see Figure 1.1; Brückner *et al.* 2000; Kwok *et al.* 2011; Horii-Hayashi *et al.* 2015). PNNs appear to have two key biological functions. First, they restrict neuronal plasticity by stabilizing synaptic connectivity, and second, they support the metabolism of highly active cell types (Karetko & Skangiel-Kramska 2009). Yet, many brain areas are rich in active cells but devoid of PNNs (Celio 1990; Crespo *et al.* 1999), and the CNS has a variety of other mechanisms to regulate neural plasticity (Nabel & Morishita 2013). So, why do some brain regions have PNNs while others do not?

PNNs emerge at the end of developmental time windows of heightened plasticity, and contribute to the maturation and maintenance of excitation/inhibition balance within neural circuits (Hensch 2005). Their enzymatic digestion deconstructs blockades to synaptic connectivity and restores juvenile-like plasticity in adult rodents (Pizzorusso *et al.* 2002; Gogolla *et al.* 2009). PNNs further support the metabolic requirements of fast-spiking, inhibitory, interneurons that express the calcium-binding protein parvalbumin (PV), which are among the most important regulators of excitation/inhibition balance in the CNS (Hensch 2005; McRae *et al.* 2007; Hu *et al.* 2014). PV cell fast-firing behavior requires a constant source of ions and a sink for reactive oxygen species generated by cellular metabolism (Härtig *et al.* 1999). The

charged glycosaminoglycan chains of PNNs solve both demands by buffering local calcium, sodium, and potassium (Morawski *et al.* 2004), and sequestering free radicals (Cabungcal *et al.* 2013). Despite conflicting evidence (Vitellaro-Zuccarello *et al.* 2001; Wegner *et al.* 2003; Mueller *et al.* 2016), this is widely cited as an explanation for why PNNs envelop up to 90% of PV cells in some brain regions (Karetko & Skangiel-Kramska 2009; Mueller *et al.* 2016).

To understand what drives PNN distributions requires considering what drives their variation, and one place to begin studying such variation is to compare systems where it occurs naturally. The few studies to observe species differences in PNNs have found evidence of both conservation and divergence. Rat and gerbil cortices show strong similarity in PNN location but differences in staining intensity and neuropil labeling (Brückner *et al.* 1994). Comparisons to the distantly related marsupial, the gray short-tailed opossum (*Monodelphis domestica*), reveal similar PNN distributions to placentals in subcortical regions, but in cortex they surround only non-PV pyramidal neurons (Brückner *et al.* 1998). In monkeys, PNNs throughout the CNS variably associate with PV cells and envelop primarily motor regions (Mueller *et al.* 2016). PNNs further take on diverse architectures, from sharply-defined reticulate structures, to diffuse "cotton wool-like" ECM that spreads into the neuropil (Wegner *et al.* 2003). These results offer enticing evidence that the brain-wide functions of PNNs are labile throughout development and evolution, but together they represent only a clustered few data points on the vertebrate phylogeny.

Sparse literature describes PNN spatial patterns, structure, or cell type associations outside of mammals and birds (Murakami *et al.* 1994; Balmer *et al.* 2009). But, because they are present throughout vertebrates, their patterns of variation may provide clues as to why some regions have them and others do not. Here, I test the hypothesis that PV cell metabolism support

is a broad, and therefore conserved function of PNNs. Alternatively, brain regions may develop PNNs primarily to regulate synaptic plasticity, in which case PV support is a secondary function. I mapped the adult distributions of aggregated ECM throughout the CNS of fish, amphibians, and reptiles, quantified parameters of their structure, and measured their association with putative fast-spiking PV cells. I found that PNNs envelop neurons in all major brain divisions, take on a striking diversity of architectures, and have highly variable associations with PV cells.

Materials & Methods

I performed triple-label immunofluorescent staining on frozen sections of animals representing three major vertebrate classes: *Poecilia reticulata* (Trinidadian guppy; Actinopterygii; *n*=6), *Rhinella yunga* (beaked toad; Amphibia; *n*=4), and *Anolis sagrei* (brown anole; Reptilia; *n*=5). For all animals, I recorded age, location of capture, full-body weight, and length. The Colorado State University Institutional Animal Care and Use Committee approved care and use of any live animals (Protocol #16-6541AA).

Poecilia reticulata

We acquired wild-caught fish from Trinidad during the year 2015 from the Garden Grove (N 10º35'21.5" W 61º21'18.8") site (collection and export permission granted by the Republic of Trinidad and Tobago, Ministry of Food Production), and maintained breeding colonies in our lab at Colorado State University. Fish developed in social housing on a 12h light: 12h dark regimen and consumed age-appropriate amounts of fish paste and brine shrimp on alternating days. I selected fish as available from second or third generation offspring of these populations. I prepared fish for immunostaining by euthanizing in overdose immersion of MS-222 (Millipore-Sigma; Darmstadt, Germany), decapitating, fixing in 4% paraformaldehyde in 0.01M phosphate

buffered saline (PBS) (Electron Microscopy Sciences; Hatfield, PA) for 4-6 hours, and cryoprotecting in 30% sucrose and 0.1% azide overnight or until heads sank.

Rhinella yunga

Our lab obtained wild-caught toads from Peru captured during the year 2015 (collection and export permits 0071-2015-SERFOR-DGFFS/DGEFFS; 195-2015-SERFOR-DGGSPFFS). Whole bodies were fixed in 4% paraformaldehyde and preserved in 70% ethanol. In preparation for immunohistochemical analysis, I decapitated toads and rehydrated heads in a decreasing ethanol/0.01M PBS solution gradient prior to cryoprotection in 30% sucrose and 0.1% azide until heads sank.

Anolis sagrei

I received wild-caught adult lizards from the Cayman Islands and Bahamas shipped live from Harvard University overnight to Colorado State University (Harvard IACUC Protocol #26-11; Collection and export permission granted by Cayman Islands Department of Environment, Bahamas Environment, Science, and Technology Commission, and Bahamas Department of Agriculture). I euthanized lizards on the day of arrival with an anesthetic dose followed by overdose of MS-222 (Millipore-Sigma), following Conroy *et al.* (2009). I decapitated heads, fixed them in 4% paraformaldehyde overnight, and cryoprotected them in 30% sucrose and 0.1% azide until heads sank. I manually extracted brains from the skull prior to sectioning.

Immunohistochemistry

I stored whole heads or dissected brains in 30% sucrose and 0.1% azide solution at 4°C until sectioning. At the time of sectioning, I flash froze head material in OCT embedding compound (Tissue-Tek; Torrance, CA) in a dry ice isopentane bath. I sectioned head material in

a cryostat at -20°C at thickness 16 μm for *P. reticulata*, 20 μm for *R. yunga*, and 50 μm for *A. sagrei*.

To visualize PNNs, I applied standard fluorescent lectin staining procedures with biotinylated *Wisteria floribunda* agglutinin (WFA; 1:500; Vector Laboratories; Burlingame, CA). WFA binds specifically to the N-acetylgalactosamine residues of the PNN hyaluronan backbone and is a widely established probe for PNNs (Brückner *et al*. 1994; 1998). To visualize parvalbumin-positive cells (PV), I used a rabbit anti-PV primary (1:1000 0.01M PBS; Invitrogen; Carlsbad, CA). For fluorescent markers, I used Streptavidin-conjugated Texas Red (1:100 0.01M PBS; Vector Laboratories) and goat anti-rabbit Alexa Fluor 488 (1:300 0.01M PBS; Invitrogen). To confirm that WFA- and PV-labeling were associated with cells and to delimit brain regions and neuronal populations, I stained cell nuclei using DAPI (1:500 0.01M PBS; Millipore-Sigma) in the secondary antibody cocktail. In brief, slides were washed three times in PBS, incubated in primary solution overnight at 4°C, washed again three times in PBS, incubated in secondary solution for two hours at room temperature, washed again three times in PBS, and coverslipped in Fluoromount-G (SouthernBiotech; Birmingham, AL). Negative controls excluded the primary or secondary antibody preparation and did not show WFA- or PV-labeling.

I photographed stained sections on an Olympus BX51 microscope (Shinjuku, Tokyo, Japan) under UV excitation wavelengths 358 nm, 488 nm, and 561 nm. Therefore, DAPI, PV, and WFA staining emitted fluorescent signal in the blue, green, and red channels respectively. I captured and merged multi-channel images with an Olympus DP71 camera and Olympus DP2-BSW acquisition software.

Sampling design

For all species, I randomly selected three images (r=3; where possible) per brain region/cell population per individual for quantification. I made effort to photograph consistently in a single brain hemisphere for a given region, except when tissue destruction, folding, or small region size precluded gathering three samples for that region, in which case region data may represent a mix of left and right hemispheres. During microphotography, I selected sections that represented the maximum cross-sectional area of the region/nucleus, such that I avoided underrepresenting the PNN population by counting at the edges of regions. I aimed to take all photos for a region in the same orientation, such that the centroid of the region was located at the center of the photograph. For wide, flattened regions (such as the anterior central grey in *P. reticulata*), I anchored photographs such that the medial edge of the region was adjacent to the edge of the photograph. I took WFA and PV photos at a constant exposure time for all images (52.99 ms for *A. sagrei* and *P. reticulata*, and 86.63 ms for *R. yunga*), except in regions of highly dense staining, where I reduced exposure times such that the brightest PNNs were distinguishable from the background. In cases of faint PV-labeling, I used a longer exposure time to provide sufficient contrast for identification.

For all species, I delimited brain regions using the atlases of Nieuwenhuys *et al.* (1998). I deemed a region PNN-positive if more than five cells were surrounded by PNNs (or if WFA-labeling was exceptionally prominent around a few cells), and absent if less than five. I used DAPI labeling to confirm region identity based on region morphology, relative position to landmarks (*e.g.* ventricles, fiber tracts, other conspicuous nuclei), and consistency within and across individuals.

Quantitative analysis of WFA-labeling

For *R. yunga* and *A. sagrei*, where WFA labeled discrete pericellular structures, I used a region of interest (ROI) approach to quantify the area and intensity of WFA staining. I used ImageJ (NIH; v1.50i) to select square ROIs such that all four borders were approximately tangent to the outer edge of WFA-labeling around the cell soma (Figure 2.1A-D). I counted a cell as PNN-positive if WFA-labeling was prominently distinguishable from background and at least two-thirds of the cell body within the focal plane of the image was surrounded by WFA staining. All visible WFA-labeled pericellular structures in each image were subject to analysis, unless they were clearly outside the boundaries of a nucleus. For these species, I measured the total size of the ROI and the average intensity of stain within the ROI to quantify PNN size and brightness. All images were processed by investigators blind to brain region.

For *P. reticulata*, exceptionally dense WFA-labeling demanded a different analysis technique. To quantify WFA-labeling, I measured the fraction of thresholded area of WFA stain covering each brain region (Figure 2.1E-H). I first outlined the total area of the cell population in WFA photographs based on DAPI staining, transformed images to 16-bit grayscale, then applied an auto-thresholding algorithm to binarize the image. The Renyi Entropy thresholding algorithm (Kapur *et al.* 1985) provided the most consistent and accurate thresholding, however in cases of strong background staining, I applied a set threshold value of 60, which gave similar results as auto-thresholding on images with low background. I then retrieved the percent area of above-threshold staining for the area of the selected region. I used the threshold value reported by the auto-thresholding algorithm as a proxy for quantification of PNN brightness as measured by intensity of WFA staining.

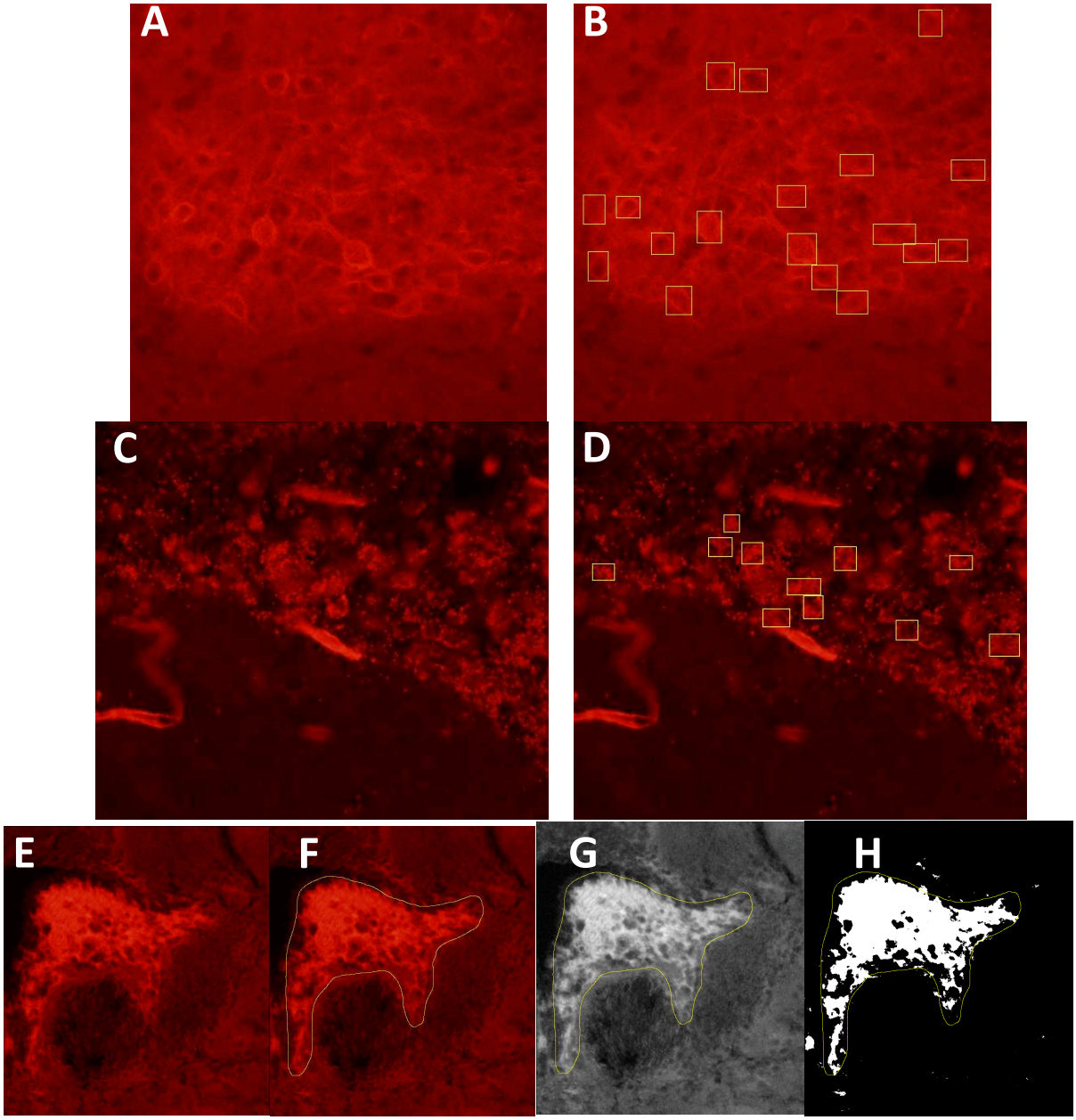

Figure 2.1. Quantification of PNNs in ImageJ. (A, B) Lateral hypothalamic area in *A. sagrei*. (C, D) Nucleus of medial longitudinal fascicle in *R. yunga.* (E-H) Periaqueductal grey in *P. reticulata.* (A, C, E) Raw images prior to analysis. (B, D) Images after completion of region of interest (ROI) selection. (F) Selection of neuronal population. (G) Transformation to 16-bit grayscale. (H) Result of auto-thresholding with Renyi Entropy algorithm (Kapur *et al.* 1985). All images taken at 200x mag.

I used the R software package (https://www.r-project.org; v3.3.1) to visualize measures of PNN size (total area of coverage in the case of *P. reticulata*), and PNN brightness.

Qualitative analysis of PNN-PV co-localization

To determine association of PNNs with PV cells, I used merged-channel images acquired as above. Because PNN-PV co-staining tended to be a many-or-none response, I characterized regions as either PV-positive or not. I counted a cell as PNN-PV if it clearly showed discernable PV labeling within the confines of WFA label (Figure 2.2A). While I observed variation in intensity of PV-staining, I did not quantify these differences. Some regions in *A. sagrei* demonstrated the presence of small pockets of PV-staining in the "gaps" of the reticulate PNN, which I interpreted as PV-positive presynaptic boutons (Figure 2.2B). Thus, these cells appeared to receive input from PV neurons. I labeled these regions "PV-in".

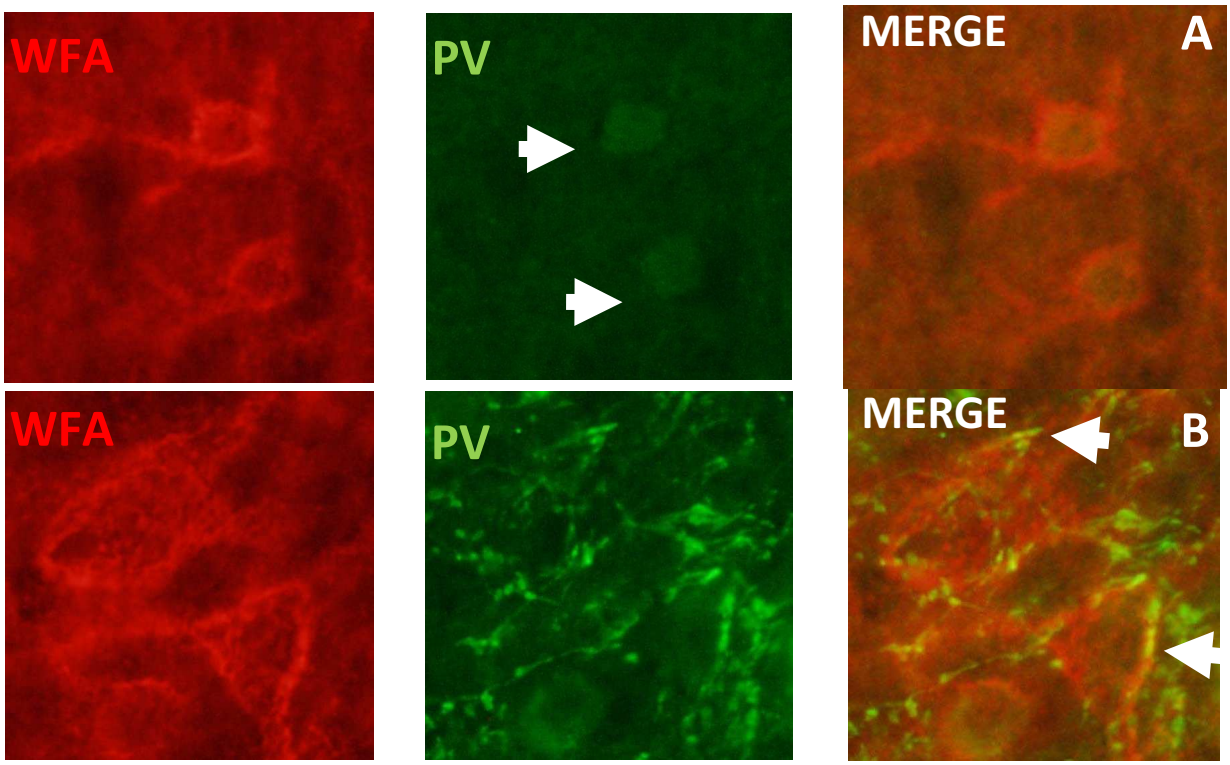

Figure 2.2. Association of PNNs with PV neurons in *Anolis sagrei.* (A) PV-PNN cells were determined with co-localization of staining, without regard to variation in stain intensity. Arrows indicate PV staining. Region is lateral hypothalamic area (Alh). (B) Some PNN cells were negative for PV staining in the cell body, but showed strong PV label in the spaces of the perineuronal net (arrows). Region is subcoerulean area (Sc). Images at 200x magnification.

Results

I found unique and diverse patterns of WFA- and PV-staining throughout the CNS of all species studied. Table 2.1 contains a summary of the major areas containing WFA-labeled ECM structures across species. Figure 2.6 summarizes distributions and PV-PNN associations for all species.

Table 2.1. Distributions of PNNs across vertebrates. (+) indicates presence, ( ) indicates absence. Presence determined by observation of at least five PNNs or prominent staining in a brain region. *Mus musculus* data from [1]Seeger *et al.* (1994), [2]Brückner *et al.* (2000), [3]Miyata *et al.* (2004), [4]Costa *et al.* (2007), [5]Horii-Hayashi *et al.* (2015).

Region	*P. reticulata*	*R. yunga*	*A. sagrei*	*M. musculus*
Septum			+	+[5]
Amygdala		+	+	+[5]
Suprachiasmatic nucleus		+	+	+[3]
Dorsal hypothalamus	+	+	+	+[4]
Ventral thalamus		+	+	+[1]
Optic tectum			+	+[5]
Nucleus of the medial longitudinal fascicle	+	+	+	+[5]
Periaqueductal grey	+			[4]
Ventral tegmental area			+	+[5]
Reticular formation	+	+	+	+[5]
Locus coeruleus			+	[4]
Vestibular nuclei	+	+	+	+[5]
Cranial nerve nuclei	+	+	+	+[5]
Cerebellum			+	+[3]

Poecilia reticulata

Telencephalon. WFA-labeling was absent in the telencephalon.

Diencephalon. WFA-labeling was present in the dorsal hypothalamus.

Mesencephalon. WFA strongly labeled pericellular structures in the nucleus of the medial longitudinal fascicle.

Medulla. WFA strongly labeled pericellular structures in the periaqueductal (central) grey matter. WFA-labeling was absent in the cerebellum. WFA labeled dense ECM in reticular and cranial nerve nuclei of the medulla (Figure 2.6A).

PNN structure.

In the dorsal hypothalamus, WFA labeled dense ECM in the center of neuronal populations that I interpreted as neuropil, which spread to surround the innermost layer of cell bodies. In the nucleus of the medial longitudinal fascicle and the periaqueductal grey, WFA stained a dense layer of ECM, surrounding neurons but also spreading thickly into the space between DAPI-labeled nuclei, comprising a "field" of WFA-labeled ECM, with cells scattered throughout (Figure 2.3A). In the reticular and cranial nerve nuclei, PNNs resembled the discrete perineuronal staining pattern observed in mammals, but with notable diffuse spillover into the neuropil. The fraction of region area covered by WFA stain was greatest in the nucleus of the medial longitudinal fascicle (nMLF) and the periaqueductal, or central, grey (CG) (Figure 2.3B). Brightness of PNNs, as measured by threshold values of WFA staining, was largely consistent across brain regions (Figure 2.3C).

Association with PV cells. PV-staining labeled PV neurons throughout the CNS, however only in the brainstem reticular and cranial nerve nuclei did I observe PNN-PV co-labeling. PNNs in the dorsal hypothalamus, nucleus of the medial longitudinal fascicle, and periaqueductal grey were devoid of PV cells in all individuals (Figure 2.6A).

Rhinella yunga

Telencephalon. WFA-labeling was present in the medial pallium, and the medial and lateral amygdala.

Diencephalon. WFA-labeling was strongly present in the ventrolateral thalamus, and the suprachiasmatic nucleus, posterior tuberculum, and dorsal regions of the hypothalamus.

Mesencephalon. WFA labeled structures in the nucleus of the medial longitudinal fascicle. Rarely, I observed WFA staining in the principal nucleus of the torus semicircularis.

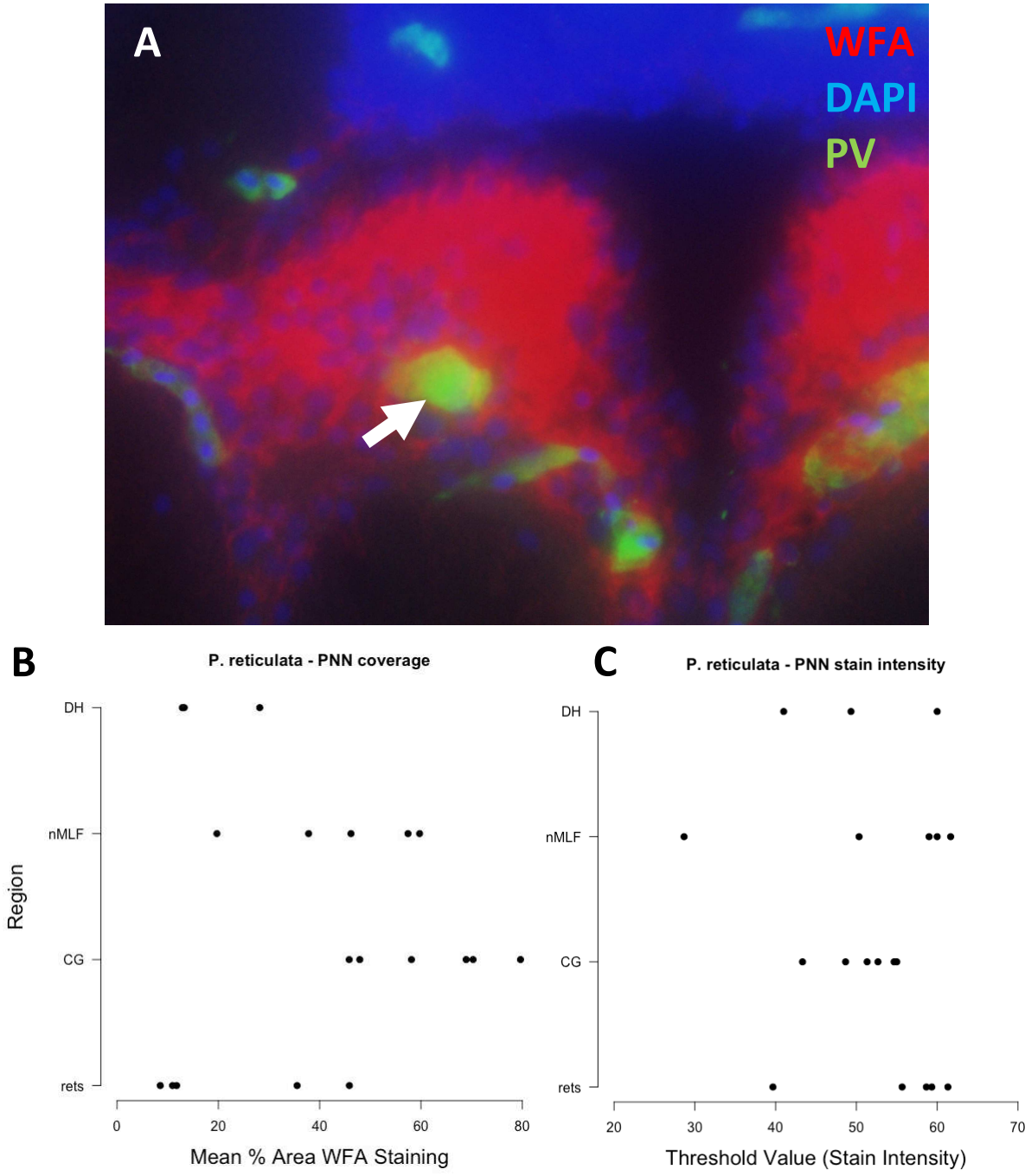

Figure 2.3. Perineuronal nets in *P. reticulata*. (A) Field-like PNNs in *P. reticulata* periaqueductal grey. Note cell nuclei (blue; DAPI) interspersed among dense ECM (red; WFA), and blood vessel labeling by PV (green) (630x magnification). (B) Fraction of region area covered by above-threshold PNN stain. (C) Thresholded value of PNN stain intensity. (B-C) Each point is the average across reps for one individual for a given brain region. Anterior/forebrain regions topmost, posterior/hindbrain regions bottommost.

Medulla. WFA labeled structures in the brainstem reticular and cranial nerve nuclei (Figure 2.6B).

PNN structure. In contrast to the reticulate form typical of PNNs, WFA staining in this species was characterized by a "granular" pattern reminiscent of immature PNNs in mammals (Figure 2.1C; Brückner *et al.* 2000). WFA-staining resulted in clusters of small, brightly-stained spheres that surrounded the perimeter of cell bodies. Often these sphere clusters were localized to one side of the cell body. Many of these clusters were associated with a field of weaker WFA stain around the cell, sometimes extending and filling into the spaces between cells (Figure 2.4A). Sizes of PNNs and WFA stain intensity did not vary strongly within and across brain regions (Figures 2.4B and 2.4C).

Association with PV cells. I found weak association of PNNs with PV-staining only in the brainstem reticular and cranial nerve nuclei (Figure 2.6B). PNNs occasionally seemed to associate with a few large PV cells in these regions, but did not envelop the entirety of the cell body.

Anolis sagrei

Telencephalon. WFA-labeling revealed a small number of densely-staining PNNs around soma, axons, and dendrites of neurons in the lateral septum, the supraoptic nucleus, and the bed nucleus of the stria terminalis.

Diencephalon. WFA labeled PNNs in the ventrolateral, medial, and lenticular nuclei of the thalamus, and the lateral hypothalamic area.

Mesencephalon. WFA labeled PNNs in the optic tectum, the nucleus of the medial longitudinal fascicle, the ventral tegmental area, and rarely in the central nucleus of the torus semicircularis.

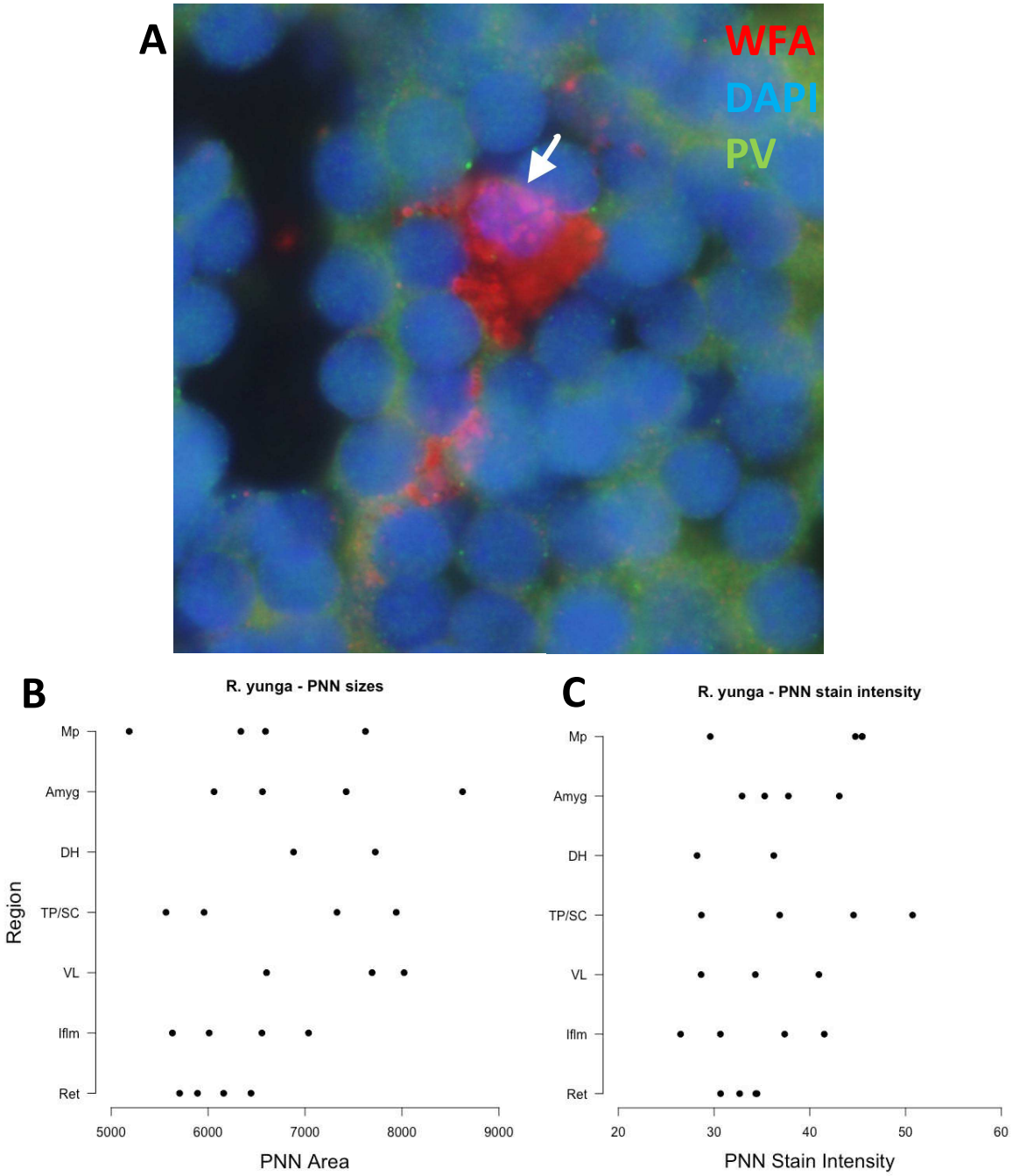

Figure 2.4. Perineuronal nets in *R. yunga*. (A) Granular, possibly immature, PNNs in *R. yunga* brainstem reticular nuclei. Note cell nucleus (arrow; blue; DAPI) covered by extensive ECM (red; WFA), and background PV staining (green) (630x mag.). (B) Average sizes of PNNs in each region. (C) Intensity of PNN stain in each region. (B-C) Each point is the average across reps for one individual for a given brain region. Anterior/forebrain regions topmost, posterior/hindbrain regions bottommost.

Medulla. WFA labeled numerous large cells in the brainstem reticular formation, including the raphe nuclei. WFA densely labeled cells in the locus coeruleus, subcoerulean area, lateral lemniscus, vestibular nuclei, and cranial nerve motor nuclei. WFA-labeled nets surrounded most PV-positive Purkinje neurons in the cerebellum (Figure 2.6C).

PNN structure. PNNs in this species were discrete, reticular structures reminiscent of mammalian PNNs (Figure 2.5A). Many regions contained defined PNNs with bright borders, whereas others showed distinct spread into the neuropil or along neuronal processes, making individual cell bodies difficult to identify. In the locus coeruleus, WFA labeled the boundaries of large cells, as well as the neuropil which gave the appearance of a rough-textured field of ECM. PNN size (Figure 2.5B) and staining intensity (Figure 2.5C) both varied across brain regions.

Association with PV cells. I found variable association of PNNs with PV cells throughout the brain, as well as regions in which PV-labeling occurred in the "gaps" of the PNN, indicating PNN-enveloped cells receiving input from PV cells (Figure 2.6C). These results are summarized in Table 2.2.

Discussion

Variation in PV-PNN association

I found that, across species, PNN associations with PV cells varied widely. In *P. reticulata* and *R. yunga*, only the brainstem reticular and cranial nerve nuclei showed PNN-PV co-staining. In *A. sagrei*, PNNs and PV cells associated in the thalamus, midbrain, and some reticular, vestibular, and cranial nerve nuclei. These regions comprise fewer than half of all regions in which I found PNNs, therefore I cannot conclude that PNN-PV associations are broad, conserved features of PNNs across vertebrates.

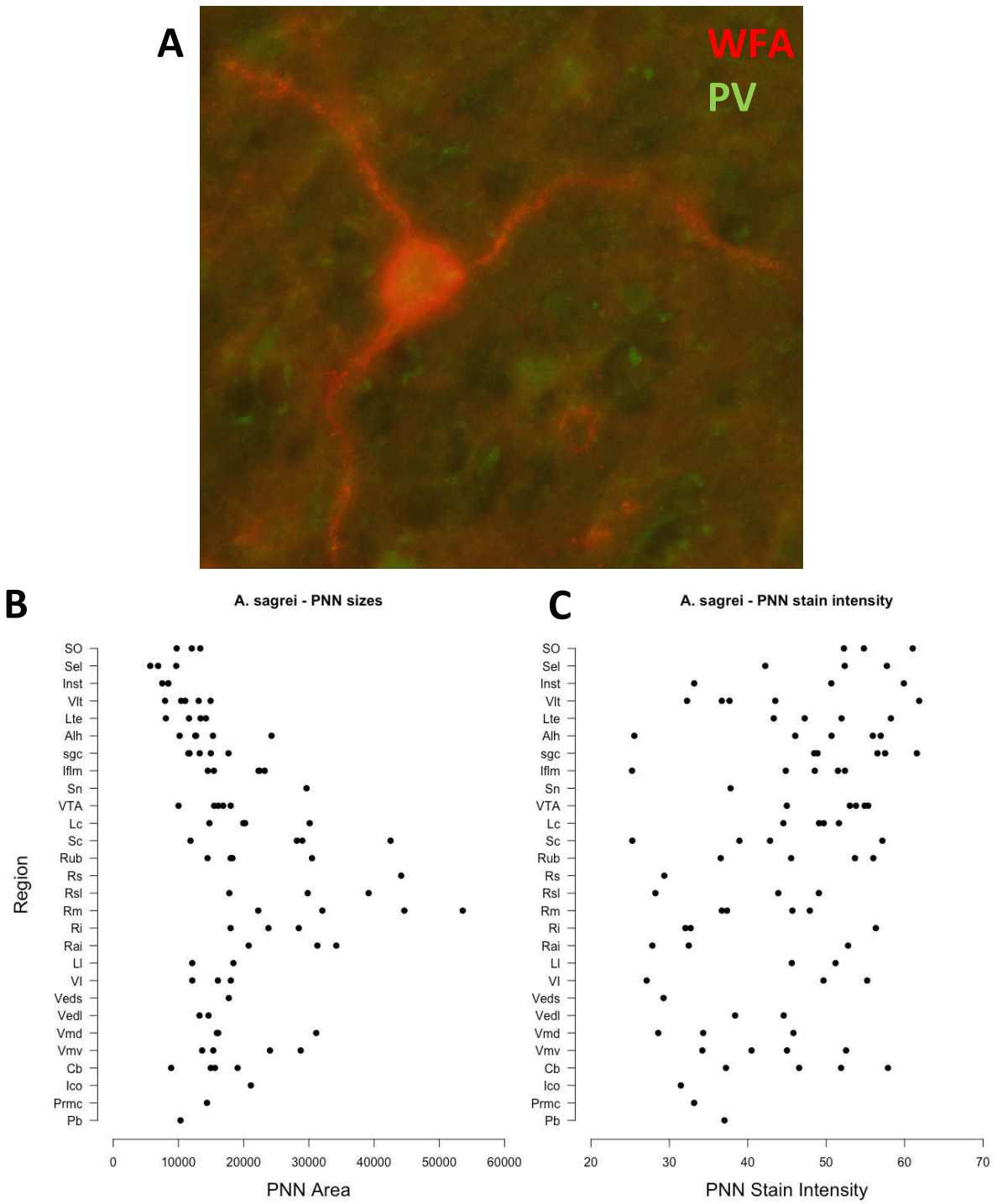

Figure 2.5. Perineuronal nets in *A. sagrei*. (A) Reticulate PNN in *A. sagrei* nucleus of medial longitudinal fascicle. Note lattice-like pericellular staining (red; WFA) around cell body and nearby processes. While obscured by dense WFA-staining in this image, this cell is PV-positive (630x magnification). (B) Average sizes of PNNs in each region. (C) Intensity of PNN stain in each region. (B-C) Each point is the average across reps for one individual for a given brain region. Anterior/forebrain regions topmost, posterior/hindbrain regions bottommost.

Table 2.2. Association of PV with PNNs in *A. sagrei*. (+) indicates PV-WFA co-labeling. Presence determined by at least one of three representative images showing robust PV-WFA co-labeling. (in) indicates PNN cell receiving input from PV-positive presynaptic bouton.

	Individual				
Region	BC1♂	BC3♂	LC1♀	UK1♀	UK2♀
SO					
Sel					
Inst					
Vlt		+			
Lte		+	+		+
Alh		+			+
sgc	+	+	+		+
Iflm		+	+	+	+
Sn	+				
VTA	+	+	+	+	+
Lc		+		+	
Sc	in	in	in	in	
Rub		+	+		
Rs	+				
Rsl	+	+		+	
Rm					
Ri					
Rai	+	+	+		
Ll		in			
VI	+	+	+		
Veds			+		
Vedl					in
Vmd	in		in	in	
Vmv	+	+		+	
Cb	+	+	+	+	+
Ico	+				
Prmc	+				
Pb					

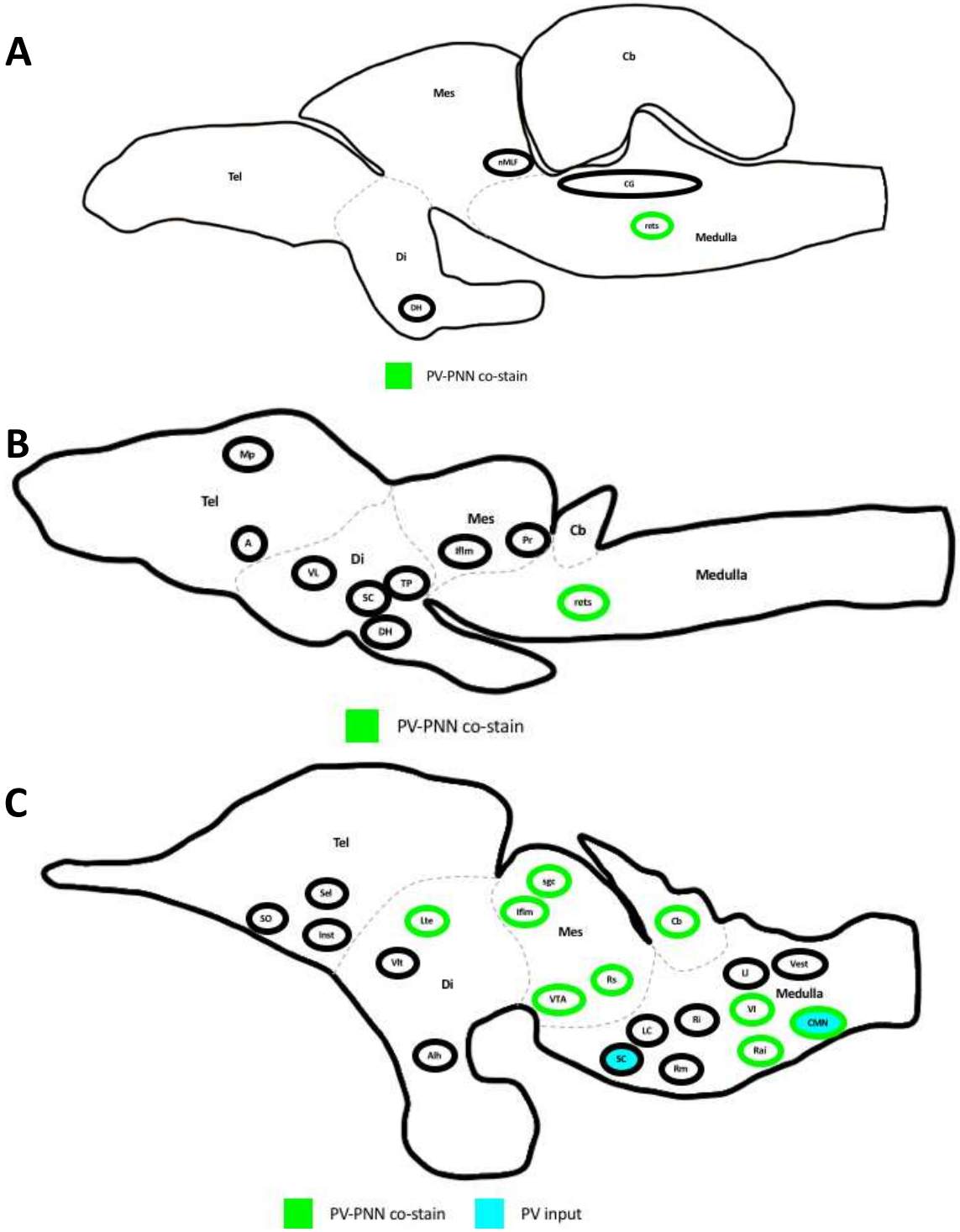

Figure 2.6. PNN and PNN-PV co-staining across adult vertebrates. Images are sagittal brain sections, with anterior/rostral at leftmost, and posterior/caudal at rightmost, collapsed along the medial-lateral axis. Dashed lines roughly define borders between major regions. Black circles indicate regions containing PNNs. Green-outlined circles represent areas with PNN-PV co-labeling. Cyan-filled circles contain PNN cells receiving PV presynaptic input. (A) *P. reticulata.* (B) *R. yunga.* (C) *A. sagrei*. Tel, telencephalon; Di, diencephalon; Mes, mesencephalon; Cb, cerebellum.

There is strong evidence that PNNs contribute to the prolonged bursting behavior of PV cells by buffering the ionic microenvironment and providing a sink for reactive oxygen species (Ohyama & Ojima 1997; Härtig *et al.* 1999; Cabungcal *et al.* 2013; Balmer 2016). However, most regions with PNNs in the animals I studied do not express PV, and I observed abundant PV cells without PNNs. I suggest that cellular metabolism support may be a novel role for PNNs, while their original role in nervous system function may have been as a regulator of synaptic plasticity. Alternative explanations for the lack of co-staining include fast-spiking behavior without expression of PV (Celio 1990), or that PV-positive neurons in other vertebrates are not fast-spiking. Future studies could determine the firing properties of PNN cells in non-PV regions using electrophysiological recordings or more general markers of cellular metabolism, such as cytochrome oxidase activity (Hevner *et al.* 1995).

I observed that the subcoerulean area and the dorsomedial nucleus of the trigeminal nerve in *A. sagrei* contained PNN cells receiving PV presynaptic input. Whether these cells are interneurons or projection neurons remains unknown, but in either case this finding of PNN cells as targets of PV input differs from the current picture of PNN cells as generators of PV output. Crook *et al*. (2007) found similar results in the macaque cerebellum, with PNN cells as targets of inhibitory output associated with cells expressing the calcium-binding protein calbindin, though they did not stain for PV. By regulating the level of inhibitory input, I speculate that PNNs in these regions could protect the firing output of their associated cells from over-inhibition, thereby regulating synaptic plasticity rather than supporting metabolism of their neurons.

Conservation in PNN expression

In all species, I found PNNs in the nucleus of the medial longitudinal fascicle (here, "nMLF"), and the brainstem reticular nuclei. PNNs associated with PV cells in these regions

only in some reticular nuclei, and in the nMLF of *A. sagrei*. The nMLF is a pre-motor region that sends burst signals to motoneurons that direct eye movement and spinal control in mammals (Wada *et al.* 1996; Horn *et al.* 2003), and tail locomotion in zebrafish and *Xenopus* (Nordlander *et al.* 1985; Thiele *et al.* 2014). In the monitor lizard, projections between the nMLF and vestibulo-oculomotor and vestibulospinal regions suggest similar head and eye control (ten Donkelaar *et al.* 1985). Horn *et al.* 2003 did not quantify the total proportion of PNN-enveloped cells in this nucleus in macaques and humans, but did show that all cells expressing either PV or calretinin (another marker of putative fast-spiking neurons) co-stain with PNNs. Similarly, in cats, this region is associated with dense cytochrome oxidase activity, indicative of cellular metabolism (Chen & May 2002). Again, due to PNN-PV variability I observed across species, I speculate that nMLF PNNs primarily stabilize inputs to neurons in this region, with support of PV cells as a possible co-opted function.

The only regions I found to consistently express both PNNs and associated PV neurons were the brainstem reticular nuclei. Steullet *et al.* (2017) found PNN-PV associations in both human and mouse reticular nuclei, and found that genetic knockout mice for an enzyme involved in antioxidant production exhibited decreases in PV cell counts and decreased bursting output from those cells, supporting a role in cellular metabolism. Due to the observed conservation of PNN-PV co-expression across species and evidence of metabolic support in mammals, future electrophysiological studies combined with PNN removal could disentangle the relative roles of synaptic stabilization and metabolic support in these interesting nuclei.

Divergence in PNN expression

I found that PNNs take on a variety of staining patterns, intensities and sizes across species and brain regions. PNNs are clearly a heterogeneous class of ECM structures, and while

many of their core components have been well-described (Miyata & Kitagawa 2017), future work should address how interactions between these components determines PNN architecture. For example, Brückner *et al.* (2000) found that tenascin-knockout mice have PNNs that persist in an immature, granular state. Carulli *et al.* (2010) likewise found that cartilage link protein knockout mice have attenuated PNNs. My characterization of PNN structural diversity suggests that PNN capacity to regulate plasticity or support metabolism could vary across brain regions.

In *P. reticulata*, I found that WFA labeled unusually dense field-like ECM in the nMLF and central, or periaqueductal, grey (here, "PAG"). The PAG is implicated in defensive behaviors in mammals (Assareh *et al.* 2016; Deng *et al.* 2016) and vocal signaling a species of fish (Kittelberger *et al.* 2006; Kittelberger & Bass 2013). Due to prominent WFA-labeled ECM in the PAG of this species, guppies represent an interesting system to explore both the roles of PNNs in plasticity of behavior, as well as molecular processes that drive PNN structure. I also noted that the nMLF and PAG are situated adjacent to the ventricle, and speculate that this dense field of ECM could regulate diffusion of ions and molecules from the cerebral spinal fluid. However, why dense ECM selectively surrounds these and not other exposed regions is unclear.

In *R. yunga*, I found that PNNs took on a granular structure reminiscent of immature PNNs in mammals (Brückner *et al.* 2000). While this result contrasts the observations of Matesz *et al.* (2005) in the brainstem and spinal cord of *Rana*, who observed discrete pericellular structures, they targeted the specific PNN components hyaluronan, tenascin C, phosphacan, fibronectin, and laminin. They did not stain with WFA, which binds the N-acetylgalactosamine residues of the hyaluronan backbone of the PNN. One interpretation of this difference is that *R. yunga* PNNs have a different arrangement of chemical components. My observations are more in line with Gaál *et al.* (2014), who found a similar pattern of small, bright spheres of WFA staining

in the cerebellar neuropil of *Rana esculenta*. While they observed WFA-staining only in the neuropil, I observed clear pericellular concentrations of WFA stain throughout the CNS, indicative of possibly immature PNNs. One alternative interpretation is that dehydrating the tissue in ethanol altered PNN staining, however the consistency of my results between individuals suggests that WFA accurately indicates regions containing PNNs.

In *A. sagrei*, the reticulate, lattice-like PNN structure resembled that seen typically in mammals. One interesting exception was the locus coeruleus, where I observed intense WFA-staining in the neuropil that was difficult to visually distinguish from pericellular concentrations of stain typical of PNNs. This region, in mammals as well as reptiles, is a catecholaminergic neuromodulatory center that generates switches in behavioral states in response to unexpected stimuli (Lopez *et al.* 1992; Bouret & Sara 2005). Due to the intense WFA-staining I observed in this species, I speculate that PNNs and ECM could stabilize synaptic inputs into this region, thereby fixing responses to salient stimuli that are established during early-life experience.

Summary

Spatial and structural diversity characterize vertebrate PNNs. Their regional distributions and variation in size and intensity suggest they are broadly poised to regulate CNS plasticity in diverse neuronal populations. Their support of PV cell metabolism, while not understated in importance, is region- and lineage-specific and may represent an adaptive evolutionary co-option of structures already involved in regulating synaptic plasticity.

CHAPTER 3: DIVERSE DEVELOPMENTAL TRAJECTORIES OF PERINEURONAL NETS

Introduction

The properties of neurons that dictate animal behavior confer the capacity for learning and memory by being both capable of updating (*plasticity*) and maintaining reliable patterns of activity (*stability*). Yet, while youth is characterized by great plasticity, maturity is dominated by stability. What, then, regulates the balance of neural plasticity and stability over an animal's lifetime? Recent years have seen the neural extracellular matrix (ECM) as a key player in maintaining plasticity/stability balance over development (Celio *et al.* 1998; Takesian & Hensch 2013; Miyata & Kitagawa 2017). In contrast to the loose, diffuse neural ECM, structured, lattice-like ECM compounds envelop various neuronal subtypes in specific brain regions during development (Wegner *et al.* 2003). Cells expressing the membrane-bound protein hyaluronan synthase secrete a hyaluronic acid chain into the extracellular space, which binds chondroitin sulfate proteoglycans, link proteins, and tenascins to create a thick, organized, web of coating around neuronal soma and nearby processes, known as the perineuronal net (PNN) (Kwok *et al.* 2011).

A key feature of PNNs is that they are physical and chemical blockades for approaching axons (Carulli *et al.* 2013; Vo *et al.* 2013; Sorg *et al.* 2016). The emergence of PNNs in a brain region closes windows of activity-dependent rewiring and is indicative of a mature circuit component (Hockfield *et al.* 1990; Hensch 2005; Bikbaev *et al*. 2015). Experiments digesting PNNs with the enzyme chondroitinase ABC support a causal role in circuit stabilization, resulting in a return to juvenile levels of plasticity and learning capacity in adult rodents (Pizzorusso *et al.* 2002; Gogolla *et al.* 2009; Wang *et al.* 2011; Hylin *et al.* 2013; Romberg *et al.*

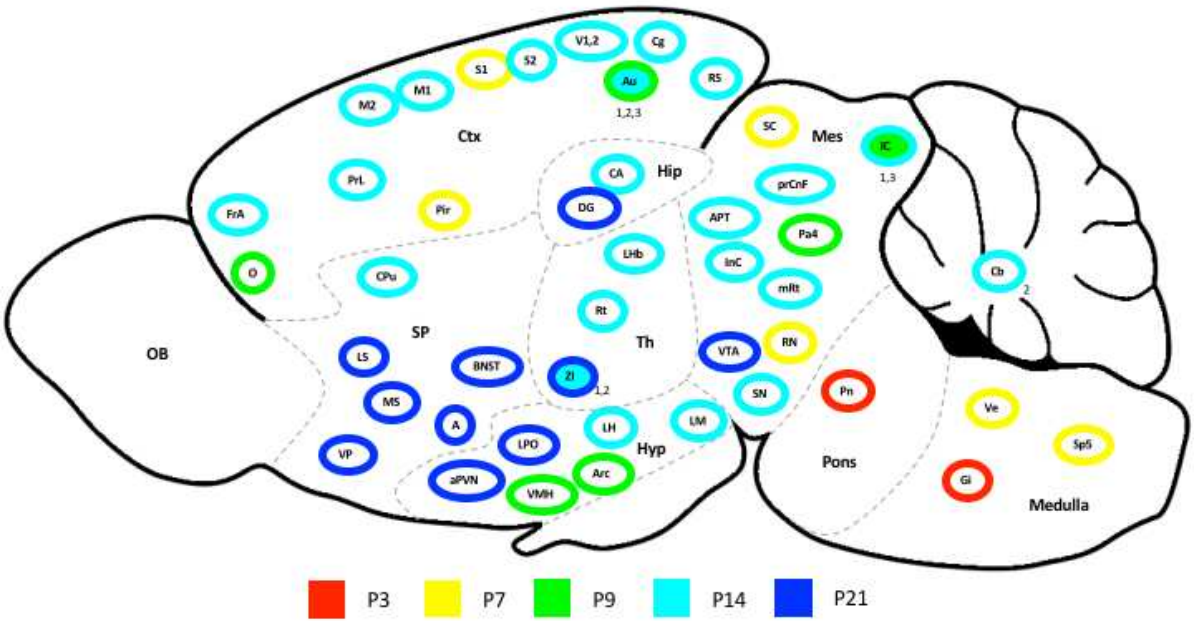

Figure 3.1. First appearance of PNNs in mouse, *Mus musculus*. P# indicates postnatal day. Based on (1) Horii-Hayashi *et al.* (2015), (2) Brückner *et al.* (2000), and (3) Friauf (2000). Circles with two colors indicate author disagreement, however there was strong consensus among authors. Sagittal view with PNN-containing regions positioned roughly into major brain divisions, collapsed along medial-lateral axis, using Allen Brain Atlas (2008). Anterior/rostral regions leftmost, posterior/caudal regions rightmost. OB, olfactory bulb; Ctx, cortex; SP, subpallium; Hip, hippocampus; Th, thalamus; Hyp, hypothalamus; Mes, mesencephalon; Cb, cerebellum. See Table 1.1 for region abbreviations.

2013; Happel *et al.* 2014). PNNs have therefore earned the suitable title of "molecular brakes" on developmental neural plasticity (Nabel & Morishita 2013).

Mammalian and avian literature points to a wide and regulated spatiotemporal distribution of PNNs. In rodents and primates, they are present throughout cortical, subcortical, and diencephalic regions, brainstem, and spinal cord (Brückner *et al*. 1994; 1998; Bertolotto *et al*. 1996; Mueller *et al*. 2016). Roughly, PNNs develop from medullar to sensory input nuclei, then progress to higher association regions in the cortex and subpallium (Figure 3.1) (Brückner *et al.* 2000; Friauf 2000; Horii-Hayashi *et al.* 2015). PNNs develop postnatally, and in mammalian sensory and avian motor cortices require sensory experience for maturation

(Pizzorusso *et al.* 2002; McRae *et al.* 2007; Balmer *et al.* 2009; Yamada & Jinno 2013). Taken together, the role of PNNs as brakes on developmental plasticity and their pattern of expression over time from lower sensory input to higher associational regions suggests that they stabilize neural connectivity in a "ground-up" fashion. This pattern of development led Takesian & Hensch (2013) to hypothesize that PNNs establish a reliable low-level processing foundation that provides flexibility for high-level association layers, thus maintaining stable circuits as input for remaining plastic pathways.

If the ground-up model is true across vertebrates, it may represent a fundamental principle of PNN biology. If the model is unique to mammals, it may represent a key innovation in mammalian evolutionary history that facilitated the rapid evolution of complex cognitive abilities. While aggregated perineuronal structures are known to exist in other vertebrate lineages, no comprehensive or brain-wide studies examine their developmental trajectories or interpret them in context of broad features of CNS construction (Murakami *et al.* 1994; Matesz *et al.* 2005; Gaál *et al.* 2014). I therefore tested whether a progressive, ground-up circuit stabilization model inspired by mammalian research is generalizable across vertebrates.

I characterized the spatial and temporal emergence of PNNs across the CNS throughout development of fish, amphibians, and reptiles. I found a striking diversity of spatial distributions, as well as temporal differences in PNN expression. Broadly, PNNs, in contrast to the ground-up model, emerge first in fore- and mid-brain regions responsible for modulating behavioral states, and only later develop in lower processing regions that route incoming sensory and outgoing motor signals.

Materials & Methods

The methods reported here largely parallel those described in Chapter 2, but I will repeat some details here for clarity, along with additional information pertinent to this experiment. I performed double-label fluorescence lectin staining on frozen sections of animals of varying developmental ages in species representing three major vertebrate classes: *Poecilia reticulata* (Trinidadian guppy; Actinopterygii), *Rhinella yunga* (beaked toad; Amphibia), and *Anolis sagrei* (brown anole; Reptilia).

Poecilia reticulata

I selected fish as available from second or third generation offspring of the populations described in Chapter 2. I prepared fish for immunostaining by euthanizing in overdose immersion of MS-222 (Millipore-Sigma; Darmstadt, Germany), decapitating, fixing in 4% paraformaldehyde in 0.01M phosphate-buffered saline (PBS) (Electron Microscopy Sciences; Hatfield, PA) for 4-6 hours, and cryoprotecting in 30% sucrose and 0.1% azide overnight or until heads sank. I studied fry (<2 days old; n=4), 3-week-olds (n=3), 5-week-olds (n=6), and sexually mature adults (>130 days old; n=6).

Rhinella yunga

Our lab obtained wild-caught toads, tadpoles, and individuals in metamorphic transition as described in Chapter 2. Whole bodies were fixed in 4% paraformaldehyde in 0.01M PBS and preserved in 70% ethanol. In preparation for immunohistochemical analysis, I decapitated animals and rehydrated heads in a decreasing ethanol/0.01M PBS solution gradient prior to cryoprotection in 30% sucrose and 0.1% azide until heads sank. I studied individuals in late metamorphic climax (n=3; Gosner (1960) stages 40-44), toads aged six weeks (n=2), and two months (n=2) post-metamorphosis. We found recently that PNNs undergo rapid deconstruction

during early metamorphosis (unpublished observations), therefore I used late metamorphic climax as a baseline measure for PNN circuitry relevant to the toad life stage.

Anolis sagrei

I obtained wild-caught lizards, and offspring bred from these individuals as described in Chapter 2. I euthanized lizards on the day of arrival with an anesthetic dose followed by overdose of MS-222 (Millipore-Sigma), following Conroy *et al.* (2009). I decapitated heads, fixed them in 4% paraformaldehyde in 0.01M PBS overnight, and cryoprotected them in 30% sucrose and 0.1% azide until heads sank. I manually extracted adult and sub-adult brains from the skull prior to sectioning. I studied hatchlings (2 days old; *n*=2 unknown sex), juveniles (30-45 days old; *n*=4 unknown sex), sub-adults (127-187 days old; *n*=4 males), and adults (>1 year old; *n*=2 males, 3 females).

Immunohistochemistry

For this component of the experiment, I used the same immunohistochemically prepared slides as described in Chapter 2. In brief, I flash froze heads in OCT embedding compound (Tissue-Tek; Torrance, CA) and sectioned head material at -20°C in a cryostat at thickness 16 μm for *P. reticulata*, 20 μm for *R. yunga*, and 50 μm for *A. sagrei*. To visualize PNNs, again, I applied the biotinylated lectin *Wisteria floribunda* agglutinin (WFA; 1:500 0.01M PBS; Vector Laboratories; Burlingame, CA), which binds specifically to the N-acetylgalactosamine residues of the PNN hyaluronan backbone (Brückner *et al*. 1994; 1998). As a fluorescent marker, I used Streptavidin-conjugated Texas Red (1:100 0.01M PBS; Vector Laboratories). To confirm that WFA-labeling was associated with cells and to delimit brain regions and neuronal populations, I stained for cell nuclei using DAPI (1:500 0.01M PBS; Millipore-Sigma) in the secondary

antibody cocktail. I described the slide preparation protocol in Chapter 2. Negative controls excluded the primary or secondary antibody preparation and did not show WFA-labeling.

I photographed stained sections on an Olympus BX51 microscope (Shinjuku, Tokyo, Japan) under UV excitation wavelengths 358 nm and 561 nm. Therefore, DAPI and WFA staining emitted fluorescent signal in the blue and red channels respectively. I captured and merged multi-channel images with an Olympus DP71 camera and Olympus DP2-BSW acquisition software.

Sampling design

The sampling design here follows that described in Chapter 2. For all species, I randomly selected three images (r=3; where possible) per brain region/cell population per individual for quantification. I made effort to photograph consistently in a single brain hemisphere for a given region, except when tissue destruction, folding, or small region size precluded the gathering of three samples for that region, in which case region data may represent a mix of left and right hemispheres. During microphotography, I selected sections that represented the maximum cross-sectional area of the region/nucleus, such that I avoided underrepresenting the PNN population by counting at the edges of regions. I aimed to take all photos for a region in the same orientation, such that the centroid of the region was located at the center of the photograph. For wide, flattened regions (such as the anterior central grey in *P. reticulata*), I anchored photographs such that the medial edge of the region was adjacent to the edge of the photograph. I took WFA photos at a constant exposure time for all images (52.99 ms for *A. sagrei* and *P. reticulata*, and 86.63 ms for *R. yunga*), except in regions of highly dense staining, where I reduced exposure times such that the brightest PNNs were distinguishable from the background.

For all species, I delimited brain regions using the atlases of Nieuwenhuys *et al.* (1998). I deemed a region PNN-positive if more than five cells were surrounded by PNNs (or if WFA-labeling was exceptionally prominent around a few cells), and absent if less than five. I used DAPI labeling to confirm region identity based on region morphology, relative position to landmarks (*e.g.* ventricles, fiber tracts, other conspicuous nuclei), and consistency within and across individuals.

Quantitative analysis of WFA-labeling

For *R. yunga* and *A. sagrei*, where WFA-labeling revealed discrete pericellular structures, I used a region of interest (ROI) approach to quantify number, area, and intensity of WFA staining. I used ImageJ (NIH; v1.50i) to select square ROIs such that all four borders were approximately tangent to the outer edge of WFA-labeling around the cell soma (see Figure 2.1A-D above). I counted a cell as PNN-positive if WFA-labeling was prominently distinguishable from background and at least two-thirds of the cell body within the focal plane of the image was surrounded by WFA staining. All visible WFA-labeled pericellular structures in each image were subject to analysis, unless they were clearly outside the boundaries of a nucleus. All images were processed by investigators blind to brain region.

For *P. reticulata*, exceptionally dense WFA-labeling demanded an overall intensity analysis, whereas cell count data were not possible. To quantify WFA-labeling, I measured the fraction of thresholded area of WFA stain covering each brain region (see Figure 2.1E-H). I first outlined the total area of the cell population in WFA photographs based on DAPI staining, transformed images to 16-bit grayscale, then applied an auto-thresholding algorithm to binarize the image. The Renyi Entropy thresholding algorithm (Kapur *et al.* 1985) provided the most consistent and accurate thresholding, however in cases of strong background staining, I applied a

set threshold value of 60, which gave similar results as auto-thresholding on images with low background. I then retrieved the percent area of above-threshold staining for the area of the selected region.

Statistical analysis

I fit PNN count and area data to a generalized linear model with a Poisson error distribution and scaled Pearson's chi-square to account for overdispersion. I compared models including developmental stage, brain region, and their interaction, as predictors using likelihood ratio testing, and performed pairwise comparisons adjusted with Tukey's HSD. I used R software including the *multcomp* package (https://www.r-project.org; v3.3.1) for statistical analysis and visualization.

Results

In all species, PNNs across the brain tended to increase in abundance throughout development. In *P. reticulata*, PNNs remained sparse during the first seven weeks of life, but increased sharply during adulthood. In *R. yunga*, PNNs increased between metamorphic climax and 2 months of age. In *A. sagrei*, PNNs increased slightly from hatchling to juvenile stages, and strongly from juvenile to subadult stages.

Regional PNN differences

For both *P. reticulata* and *R. yunga*, an additive model including brain region and developmental stage was sufficient to predict PNN percent area and count, respectively (*P. reticulata*: χ^2_{13}=146.94, p=0.144; *R. yunga*: χ^2_{16}=20.662, p=0.228). For *A. sagrei*, the interaction model between brain region and developmental stage could not be reduced to an additive model (χ^2_{53}=133.31, p=0.001), therefore, the number of PNNs in a given region depended both on region identity and developmental stage.

P. reticulata. In fish, region-specific PNN developmental trajectories largely mirrored the brain-wide pattern of sharp increase after five weeks of age and into sexual maturity. However, the magnitude of coverage increase was different between regions. All regions began at less than 10% WFA-cover, but the central, periaqueductal, grey (CG) reached coverages of over 60%, while other regions (DH, rets) reached only 10-20% (Figure 3.2A). Overall, the pattern of progression proceeded from the medullar reticular nuclei (rets), to the rest of the brain regions in which I observed them (Figure 3.2B).

R. yunga. In toads, while PNNs on average tended to increase over development, region-specific trajectories showed markedly different patterns (See Appendix Figure A1.2 for all regions). For example, PNNs in the medial pallium (Mp) appeared at the end of metamorphic climax and increased in abundance through two months post-metamorphosis. Similarly, PNNs in the principal nucleus of the torus semicircularis (Pr) were not detectable in any individuals prior to two months post-metamorphosis. In contrast, PNNs in the lateral pallium (Lp) disappeared at the end of metamorphic climax, and did not return even two months post-metamorphosis (Figure 3.3A). Overall, I detected PNNs throughout all major brain divisions early in development, however their early emergence in forebrain areas and late appearance in Pr, along with loss in other regions, contrasts a ground-up progression (Figure 3.3B).

A. sagrei. In lizards, PNNs trended toward overall increase throughout development, but the magnitude and direction of change depended on brain region (See Appendix Figure A1.3 for all regions). For example, PNN increase in the ventrolateral thalamus (Vlt) increased to mature levels by the sub-adult stage, whereas counts in the lateral septum (Sel) remained stable throughout life. In contrast, PNNs in the medial reticular nucleus (Rm) increased sharply in adults, while those in the parabrachial nucleus (Pb) only arose in adulthood (Figure 3.4A).

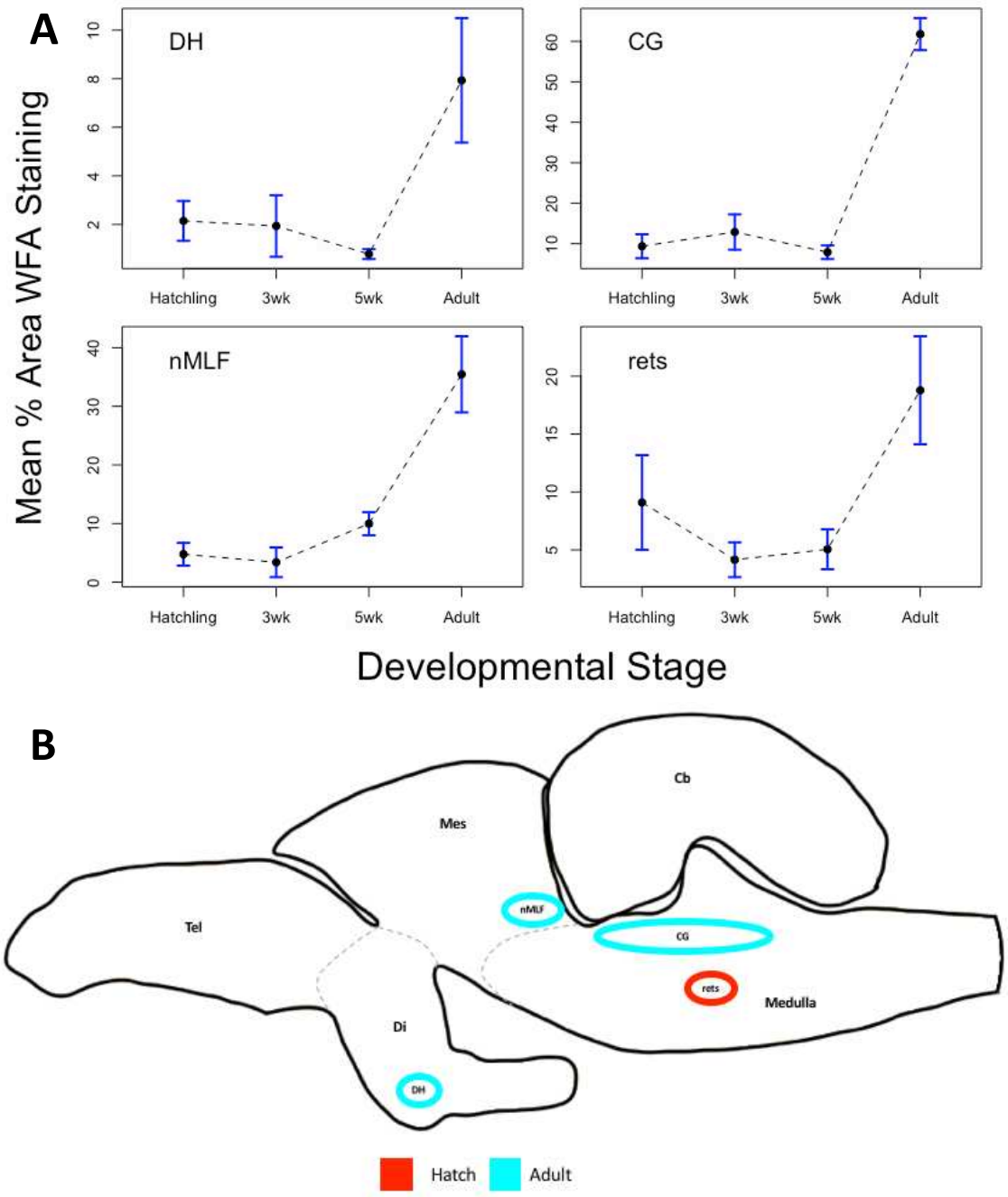

Figure 3.2. Development of PNNs by brain region in *Poecilia reticulata*. (A) Developmental trajectories by region. Means ± SEM. DH, dorsal hypothalamus; CG, central grey; nMLF, nucleus of the MLF; rets, medullar reticular nuclei. (B) Schematic of PNN development, oriented anterior/forebrain (leftmost) to posterior/hindbrain (rightmost), collapsed along the medial-lateral axis. Tel, telencephalon; Di, diencephalon; Mes, mesencephalon; Cb, cerebellum.

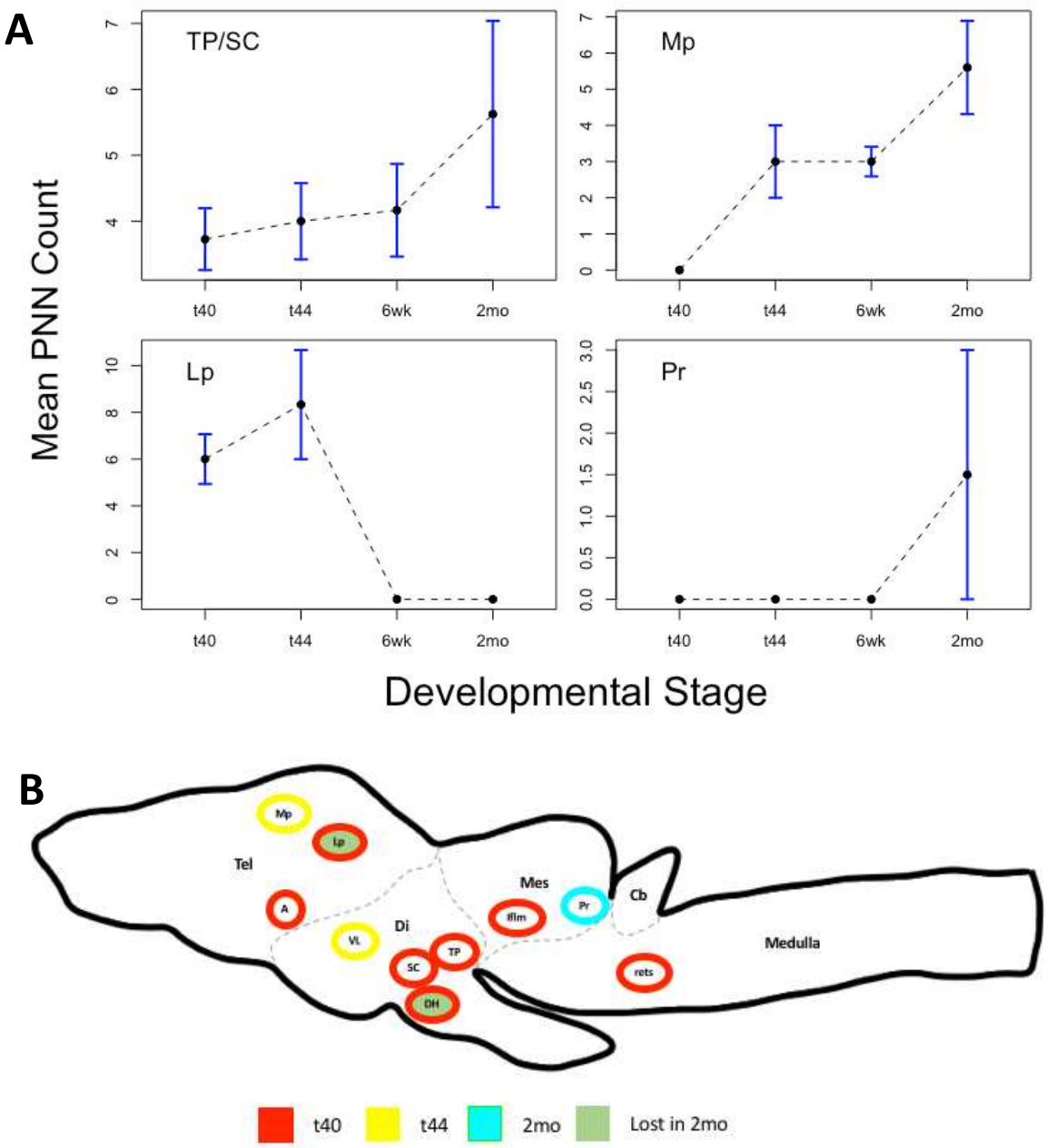

Figure 3.3. Development of PNNs by brain region in *Rhinella yunga*. (A) Developmental trajectories by region. Means ± SEM. TP/SC, posterior tuberculum/suprachiasmatic nucleus; Mp, medial pallium; Lp, lateral pallium; Pr, principal nucleus of the torus semicircularis. (B) Schematic of PNN development, oriented anterior/forebrain (leftmost) to posterior/hindbrain (rightmost), collapsed along the medial-lateral axis. Tel, telencephalon; Di, diencephalon; Mes, mesencephalon; Cb, cerebellum.

Overall, I found the earliest detectable PNNs throughout all major brain divisions except the cerebellum. The next-earliest-emerging PNNs occurred in mid- and fore-brain structures, and the cerebellum (Cb) and the nucleus of the abducens nerve (VI). Only in later development did the remaining diencephalic, mesencephalic, and medullar nuclei regions express PNNs (Figure 3.4B).

Discussion

My results show that PNNs occur with developmental trajectories that are brain region- and lineage-specific. PNNs occur broadly in diencephalic, brainstem reticular and cranial nerve nuclei, and the nucleus of the medial longitudinal fascicle. In amphibians and reptiles, PNNs extend into forebrain regions, including the medial pallium, amygdala and septal nuclei. In contrast to the mammalian model of progressive, ascending circuit stabilization, I found that PNNs emerge during development in divergent patterns across vertebrates.

Postnatal development of PNNs

While I did not manipulate animal experience, my results show that PNNs undergo substantial increases in abundance weeks after birth or hatching. Because of this developmental delay in PNN maturation, I suggest that they are poised to stabilize early-life memories that are integral to an individual's behavioral repertoire. Postnatal manipulations of animal experience show mixed effects on PNN development and behavioral plasticity. In mammalian visual and somatosensory cortices, sensory deprivation prior to PNN development leads to delayed PNN maturation and a corresponding delay in critical period closure (Pizzorusso *et al.* 2002; McRae *et al.* 2007; Nowicka *et al.* 2009; Ueno *et al.* 2017). Similarly, songbirds that lack auditory experience have delayed closure of the song-learning critical period and reduced overall PNN stain intensity (Balmer *et al.* 2009). In contrast, work in the chick visual system showed that

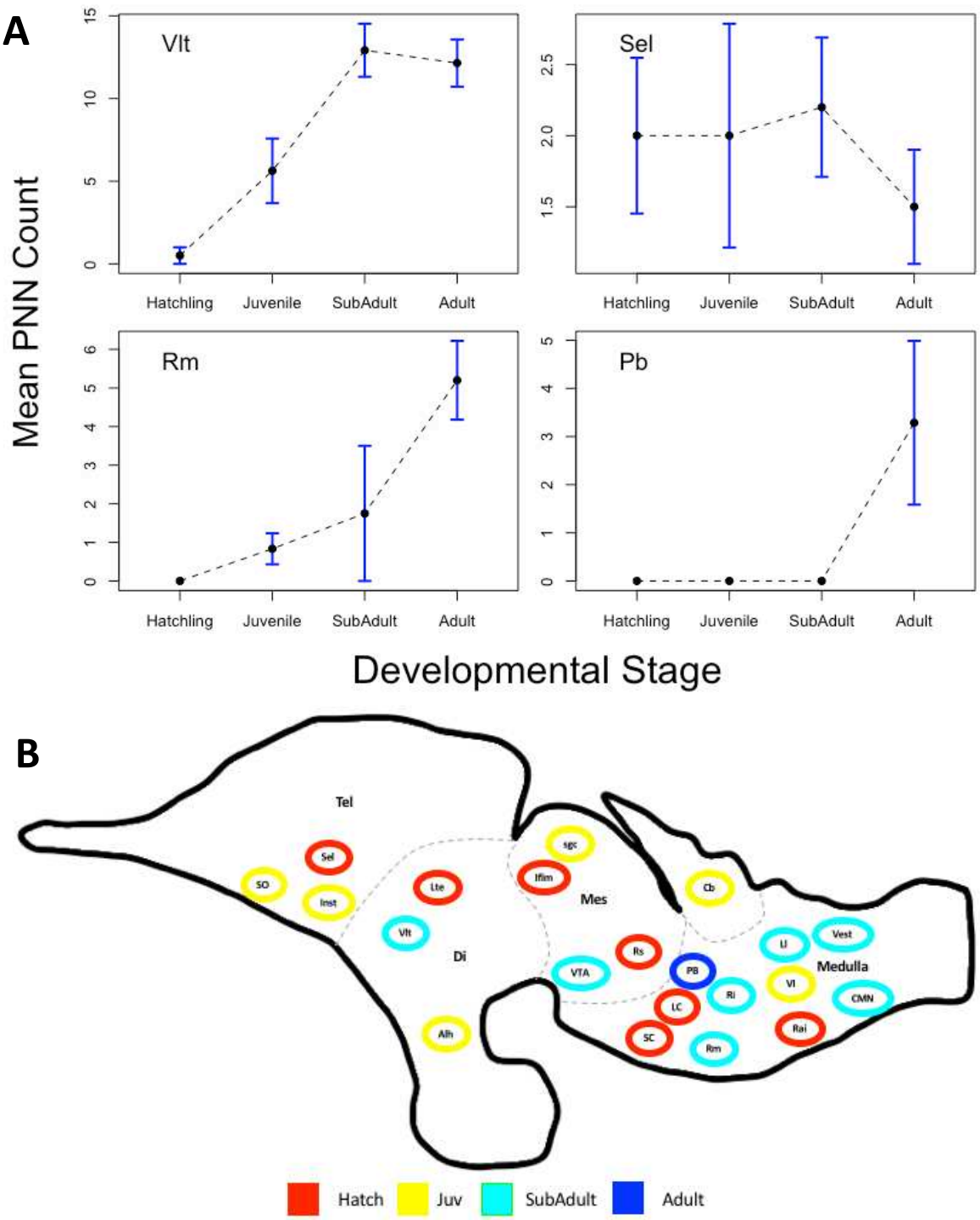

Figure 3.4. Development of PNNs by brain region in *Anolis sagrei*. (A) Developmental trajectories by region. Means ± SEM. Vlt, ventrolateral thalamus; Sel, lateral septum; Rm, medial reticular nucleus; Pb, parabrachial nucleus. (B) Schematic of PNN development, oriented anterior/forebrain (leftmost) to posterior/hindbrain (rightmost), collapsed along the medial-lateral axis. Tel, telencephalon; Di, diencephalon; Mes, mesencephalon; Cb, cerebellum.

PNNs develop regardless of sensory input (Gáti *et al.* 2010). Continued investigation linking sensory input and PNN development with the stability of their involved circuits will illuminate the extent to which PNNs are influenced by experience.

Early development of PNNs in social decision-making network regions

While I observed PNN development in brainstem nuclei as expected, I found that PNNs in forebrain processing centers emerged at the same time or earlier than many brainstem regions. In all species, I detected PNNs in some hypothalamic nuclei, and in reptiles and amphibians I found early emergence of PNNs in amygdalar and thalamic regions. In reptiles, septal PNNs formed as early as two days post-hatch, and in amphibians, PNNs formed in the medial pallium, a putative homolog of the mammalian hippocampus (González & López 2002), at the end of metamorphic climax. While the issue of homology remains under debate (Goodson & Kingsbury 2013), many of the brain regions in which I observed early PNN development comprise important nodes in the vertebrate social decision-making network (SDM). Evidence points to the SDM as a vertebrate-wide circuit responsible for determining salience of stimuli and generating adaptive motor output (O'Connell & Hofmann 2011). Why might PNNs emerge first in these regions, then later in brainstem pathways? Experiments in mammalian amygdala and hippocampus demonstrate that maintenance of early-life fear memories depend on PNN development in these regions, and that removing PNNs or genetic knockout of PNN components leads to enhanced or altered synaptic plasticity (Gogolla *et al.* 2009; Hylin *et al.* 2013; Shah & Lodge 2013; Jansen *et al.* 2017), resulting in fear memory extinction and enhanced dopamine activity. Likewise, PNNs occupy hypothalamic regions with bidirectional connectivity to the septum and known involvement in defensive behavior (Horii-Hayashi *et al.* 2017). Anterior dorsal lateral hypothalamic PNN digestion with chondroitinase similarly prevented the formation

of place preference memories driven by cocaine use in rats (Blacktop *et al.* 2017). Again, establishment of homologies in these regions, and their link to actual behavior (Hoke *et al.* 2007), is needed for non-mammalian taxa (Goodson & Kingsbury 2013). However, given PNN presence in many SDM nodes across vertebrates and their demonstrated roles in mammalian behavior, I speculate that PNNs in the SDM could stabilize early-life memories of highly salient stimuli. One possible explanation for the late development of PNNs in these regions in rodents is their limited experience during early life due to maternal care (Champagne *et al.* 2008).

Summary

The progressive, ascending, "ground-up" model of circuit stabilization by PNNs is a mode of PNN development unique to mammals. In the fish, amphibians, and reptiles studied here, PNNs follow a pattern more resembling "top-down" stabilization. Further, their developmental trajectories differ across brain regions within each species, with some regions developing PNNs late in life, whereas others are lost over time. Because the progressive, ascending, ground-up development of PNNs appears unique to mammals, one intriguing hypothesis is that this mode of circuit stabilization facilitated the evolution of complex cognitive processing in the mammalian pallium. This would imply that PNNs, or at least aggregated ECM, existed as a neuronal stabilizing mechanism in the common ancestor of all vertebrates. Key questions regarding fundamental properties of PNNs include: How dynamically regulated are PNNs over time, and what happens to neural circuits when PNNs are lost or degraded (Slaker *et al.* 2016)? And how are long-term "memories" of salient early-life events maintained by PNNs (Tsien 2013)? My results demonstrate that the species studied here offer important insight into fundamental features of PNN biology, and offer enticing, natural systems to address these remaining questions.

REFERENCES

Abbott LF, Nelson SB. **2000.** Synaptic plasticity: taming the beast. *Nature Neuroscience* **3:** 1178-1183

Allen Institute. **2008.** Allen Mouse Brain Atlas (sagittal). URL: http://mouse.brain-map.org/static/atlas

Assareh N, Sarrami M, Carrive P, McNally G. **2016.** The organization of defensive behaviors elicited by optogenetic excitation of rat lateral or ventrolateral periaqueductal gray. *Behavioral Neuroscience* **130:** 406-414

Balmer TS, Carels VM, Frisch JL, Nick TA. **2009.** Modulation of perineuronal nets and parvalbumin with developmental song learning. *Journal of Neuroscience* **29:** 12878-12885

Balmer TS. **2016.** Perineuronal nets enhance the excitability of fast-spiking neurons. *eNeuro* **3:** 1-13

Bertolotto A, Manzardo E, Guglielmone R. **1996.** Immunohistochemical mapping of perineuronal nets containing chondroitin unsulfated proteoglycan in the rat central nervous system. *Cell and Tissue Research* **283:** 283-295

Bikbaev A, Frischknecht R, Heine M. **2015.** Brain extracellular matrix retains connectivity in neuronal networks. *Nature Scientific Reports* **5:** 14527

Blacktop JM, Todd RP, Sorg BA. **2017.** Role of perineuronal nets in the anterior dorsal lateral hypothalamic area in the acquisition of cocaine-induced conditioned place preference and self-administration. *Neuropharmacology* **118:** 124-136

Bouret S, Sara SJ. **2005.** Network reset: a simplified overarching theory of locus coeruleus noradrenaline function. *TRENDS in Neurosciences* **28:** 574-582

Brückner G, Seeger G, Brauer K, Härtig W, Kacza J, Bigl V. **1994.** Cortical areas are revealed by distribution patterns of proteoglycan components and parvalbumin in the Mongolian gerbil and rat. *Brain Research* **658:** 67-86

Brückner G, Härtig W, Seeger J, Rübsamen R, Reimer K, Brauer K. **1998.** Cortical perineuronal nets in the gray short-tailed opossum (*Monodelphis domestica*): a distribution pattern contrasting with that shown in placental mammals. *Anatomy and Embryology* **197:** 249-262

Brückner G, Grosche J, Schmidt S, Härtig W, Margolis RU, Delpech B, Seidenbecher CI, Czaniera R, Schachner M. **2000.** Postnatal development of perineuronal nets in wild-type

mice and in a mutant deficient in tenascin-R. *Journal of Comparative Neurology* **428:** 616-629

Cabungcal JH, Steullet P, Morishita H, Kraftsik R, Cuenod M, Hensch TK, Do KQ. **2013.** Perineuronal nets protect fast-spiking interneurons against oxidative stress. *Proceedings of the National Academy of Sciences* **110:** 9130-9135

Carulli D, Pizzorusso T, Kwok JCF, Putignano E, Poli A, Forostyak S, Andrews MR, Deepa SS, Glant T, Fawcett JW. **2010.** Animals lacking link protein have attenuated perineuronal nets and persistent plasticity. *Brain* **133:** 2331-2347

Carulli D, Foscarin S, Faralli A, Pajaj E, Rossi F. **2013.** Modulation of semaphorin3A in perineuronal nets in the adult cerebellum. *Molecular and Cellular Neuroscience* **57:** 10-22

Celio MR, Spreafico R, De Biasi S, Vitellaro-Zuccarello L. **1998.** Perineuronal nets: past and present. *Trends in Neurosciences* **21:** 510-515

Celio MR. **1990.** Calbindin D-28k and parvalbumin in the rat nervous system. *Neuroscience* **35:** 375-475

Champagne DL, Bagot RC, van Hasselt F, Ramakers G, Meaney MJ, de Kloet ER, Krugers H. **2008.** Maternal care and hippocampal plasticity: evidence for experience-dependent structural plasticity, altered synaptic functioning, and differential responsiveness to glucocorticoids and stress. *Journal of Neuroscience* **28:** 6037-6045

Chen B, May PJ. **2002.** Premotor circuits controlling eyelid movements in conjunction with vertical saccades in the cat. *Journal of Comparative Neurology* **450:** 183-202

Conroy CJ, Papenfuss T, Parker J, Hahn NE. **2009.** Use of tricaine methanesulfonate (MS222) for euthanasia of reptiles. *Journal of the American Association for Laboratory Animal Science* **48:** 28-32

Cornez G, ter Haar SM, Cornil CA, Balthazart J. **2015.** Anatomically discrete sex differences in neuroplasticity in zebra finches as reflected by perineuronal nets. *PLoS ONE* **10:** e0123199

Cornez G, Madison FN, Van der Linden A, Cornil C, Yoder KM, Ball GF, Balthazart J. **2017.** Perineuronal nets and vocal plasticity in songbirds: a proposed mechanism to explain the difference between closed-ended and open-ended learning. *Developmental Neurobiology* **77:** 975-994

Costa C, Tortosa R, Domènech A, Vidal E, Pumarola M, Bassols A. **2007.** Mapping of aggrecan, hyaluronic acid, heparin sulphate proteoglycans and aquaporin 4 in the nervous system of the mouse. *Journal of Chemical Neuroanatomy* **33:** 111-123

Crespo C, Porteros A, Arévalo R, Briñón JG, Aijón J, Alonso JR. **1999.** Distribution of parvalbumin immunoreactivity in the brain of the Tench (*Tinca tinca* L., 1758). *Journal of Comparative Neurology* **413:** 549-571

Crook JD, Hendrickson A, Erickson A, Possin D, Robinson FR. **2007.** Purkinje cell axon collaterals terminate on Cat-301+ neurons in *Macaca* monkey cerebellum. *Neuroscience* **149:** 834-844

Deng H, Xiao X, Wang Z. **2016.** Periaqueductal gray neuronal activities underlie different aspects of defensive behaviors. *Journal of Neuroscience* **36:** 7580-7588

Friauf, E. **2000.** Development of chondroitin sulfate proteoglycans in the central auditory system of rats correlates with acquisition of mature properties. Audiology & Neuro-Otology **5:** 251-262

Gaál B, Rácz É, Juhász T, Holló K, Matesz C. **2014.** Distribution of extracellular matrix macromolecules in the vestibular nuclei and cerebellum of the frog, *Rana esculenta*. *Journal of Neuroscience* **258:** 162-173

Gáti G, Morawski M, Lendvai D, Matthews RT, Jäger C, Zachar G, Arendt T, Alpár A. **2010.** Chondroitin sulphate proteoglycan-based perineuronal net establishment is largely activity-independent in chick visual system. *Journal of Chemical Neuroanatomy* **40:** 243-247

Gogolla N, Caroni P, Lüthi A, Herry C. **2009.** Perineuronal nets protect fear memories from erasure. *Science* **325:** 1258-1261

González A, López JM. **2002.** A forerunner of septohippocampal cholinergic system is present in amphibians. *Neuroscience Letters* **327:** 111-114

Goodson JL, Kingsbury MA. **2013.** What's in a name? Considerations of homologies and nomenclature for vertebrate social behavior networks. *Hormones and Behavior* **64:** 103-112

Gosner K. **1960.** A simplified table for staging anuran embryos and larvae with notes on identification. *Herpetologica* **16:** 183-190

Happel MFK, Niekisch H, Rivera LLC, Ohl FW, Deliano M, Frischknecht R. **2014.** Enhanced cognitive flexibility in reversal learning induced by removal of the extracellular matrix in auditory cortex. *Proceedings of the National Academy of Sciences* **111:** 2800-2805

Härtig W, Derouiche A, Welt K, Brauer K, Grosche J, Mäder M, Reichenbach A, Brückner G. **1999.** Cortical neurons immunoreactive for the potassium channel Kv3.1b subunit are predominantly surrounded by perineuronal nets presumed as a buffering system for cations. *Brain Research* **842:** 15-29

Hensch TK. **2005.** Critical period plasticity in local cortical circuits. *Nature Reviews Neuroscience* **6:** 877-888

Hevner RF, Liu S, Wong-Riley MTT. **1995.** A metabolic map of cytochrome oxidase in the rat brain: histochemical, densitometric and biochemical studies. *Neuroscience* **65:** 313-342

Hockfield S, Kalb RG, Zaremba S, Fryer H. **1990.** Expression of neural proteoglycans correlates with the acquisition of mature neuronal properties in the mammalian brain. *Cold Spring Harbor Symposia on Quantitative Biology* **55:** 505-514

Hoke KL, Ryan MJ, Wilczynski W. **2007.** Integration of sensory and motor processing underlying social behaviour in túngara frogs. *Proceedings of the Royal Society B* **274:** 641-649

Horii-Hayashi N, Sasagawa T, Matsunaga W, Nishi M. **2015.** Development and structural variety of the chondroitin sulfate proteoglycans-contained extracellular matrix in the mouse brain. *Neural Plasticity* **2015:** 1-12

Horii-Hayashi N, Sasagawa T, Nishi M. **2017.** Insights from extracellular matrix studies in the hypothalamus: structural variations of perineuronal nets and discovering a new perifornical area of the anterior hypothalamus. *Anatomical Science International* **92:** 18-24

Horn AK, Brückner G, Härtig W, Messoudi A. **2003.** Saccadic omnipause and burst neurons in monkey and human are ensheathed by perineuronal nets but differ in their expression of calcium-binding proteins. *Journal of Comparative Neurology* **455:** 341-352

Hu H, Gan J, Jonas P. **2014.** Fast-spiking, parvalbumin+ GABAergic interneurons: from cellular design to microcircuit function. *Science* **345:** 1-13

Hylin MJ, Orsi SA, Moore AN, Dash PK. **2013.** Disruption of the perineuronal net in the hippocampus or medial prefrontal cortex impairs fear conditioning. *Learning and Memory* **20:** 267-273

Jansen S, Gottschling C, Faissner A, Manahan-Vaughan D. **2017.** Intrinsic cellular and molecular properties of in vivo hippocampal synaptic plasticity are altered in the absence of key synaptic matrix molecules. *Hippocampus* **27:** 920-933

Kapur JN, Sahoo PK, Wong ACK. **1985.** A new method for gray-level picture thresholding using the entropy of the histogram. *Graphical Models and Image Processing* **29:** 273-285

Karetko M, Skangiel-Kramska J. **2009.** Diverse functions of perineuronal nets. *Acta Neurobiologiae Experimentalis* **69:** 564-577

Kittelberger JM, Land BR, Bass AH. **2006.** Midbrain periaqueductal gray and vocal patterning in a teleost fish. *Journal of Neurophysiology* **96:** 71-85

Kittelberger JM, Bass AH. **2013.** Vocal-motor and auditory connectivity of the midbrain periaqueductal gray in a teleost fish. *Journal of Comparative Neurology* **521:** 791-812

Köppe G, Brückner G, Brauer K, Härtig W, Bigl V. **1997.** Developmental patterns of proteoglycan-containing extracellular matrix in perineuronal nets and neuropil of the postnatal rat brain. *Cell and Tissue Research* **288:** 33-41

Kwok JCF, Dick G, Wang D, Fawcett JW. **2011.** Extracellular matrix and perineuronal nets in CNS repair. *Developmental Neurobiology* **71:** 1073-1089

Lopez KH, Jones RE, Seufert DW, Rand MS, Dores RM. **1992.** Catecholaminergic cells and fibers in the brain of the lizard *Anolis carolinensis* identified by traditional as well as whole-mount immunohistochemistry. *Cell and Tissue Research* **270:** 319-337

Malenka RC, Bear MF. **2004.** LTP and LTD: An embarrassment of riches. *Neuron* **44:** 5-21

Matesz C, Modis L, Halasi G, Szigeti ZM, Felszeghy S, Bacskai T, Szekely G. **2005.** Extracellular matrix molecules and their possible roles in the regeneration of frog nervous system. *Brain Research Bulletin* **66:** 526-531

McRae PA, Rocco MM, Kelly G, Brumberg JC, Matthews RT. **2007.** Sensory deprivation alters aggrecan and perineuronal net expression in the mouse barrel cortex. *Journal of Neuroscience* **27:** 5405-5413

Mermillod M, Bugaiska A, Bonin P. **2013.** The stability-plasticity dilemma: investigating the continuum from catastrophic forgetting to age-limited learning effects. *Frontiers in Psychology* **4:** 1-3

Meyer CE, Boroda E, Nick TA. **2014.** Sexually dimorphic perineuronal net expression in the songbird. *Basal Ganglia* **3:** 229-237

Miyata S, Akagi A, Hayashi N, Watanabe K, Oohira A. **2004.** Activity-dependent regulation of a chondroitin sulfate proteoglycan 6B4 phosphacan/RPTPβ in the hypothalamic supraoptic nucleus. *Brain Research* **1017:** 163-171

Miyata S, Kitagawa H. **2017.** Formation and remodeling of the brain extracellular matrix in neural plasticity: roles of chondroitin sulfate and hyaluronan. *Biochimica et Biophysica Acta – General Subjects.*

Morawski M, Brückner MK, Riederer P, Brückner G, Arendt T. **2004.** Perineuronal nets potentially protect against oxidative stress. *Experimental Neurology* **188:** 309-315

Mueller AL, Davis A, Sovich S, Carlson SS, Robinson FR. **2016.** Distribution of N-acetylgalactosamine-positive perineuronal nets in the macaque brain: anatomy and implications. *Neural Plasticity* **2016:** 1-19

Murakami T, Tsubouchi M, Tubouchi Y, Taguchi T, Ohtsuka A. **1994.** The occurrence of neurons with strongly negatively charged surface coats in mammalian, avian, reptilian, amphibian and piscine brains. *Acta Medica Okayama* **48:** 195-197

Nabel EM, Morishita H. **2013.** Regulating critical period plasticity: insight from the visual system to fear circuitry for therapeutic interventions. *Frontiers in Psychiatry* **4:** 1-8

Nieuwenhuys R, ten Donkelaar HJ, Nicholson C. **1998.** *The central nervous system of vertebrates*. Berlin, Heidelberg: Springer-Verlag.

Nordlander RH, Baden ST, Ryba TMJ. **1985.** Development of early brainstem projections to the tail spinal cord of *Xenopus*. *Journal of Comparative Neurology* **231:** 519-529

Nowicka D, Soulsby S, Skangiel-Kramska J, Glazewski S. **2009.** Parvalbumin-containing neurons, perineuronal nets and experience-dependent plasticity in murine barrel cortex. *European Journal of Neuroscience* **30:** 2053-2063

O'Connell LA, Hofmann HA. **2011.** The vertebrate mesolimbic reward system and social behavior network: a comparative synthesis. *Journal of Comparative Neurology* **519:** 3599-3639

O'Leary T, Williams AH, Caplan JS, Marder E. **2013.** Correlations in ion channel expression emerge from homeostatic tuning rules. *Proceedings of the National Academy of Sciences* **110:** e2645-e2654

Ohyama J, Ojima H. **1997.** Labeling of pyramidal and nonpyramidal neurons with lectin *Vicia villosa* during postanatal development of the guinea pig. *Journal of Comparative Neurology* **389:** 453-468

Pizzorusso T, Medini P, Berardi N, Chierzi S, Fawcett JW, Maffei L. **2002.** Reactivation of ocular dominance plasticity in the adult visual cortex. *Science* **298:** 1248-1251

Romberg C, Yang S, Melani R, Andrews MR, Horner AE, Spillantini MG, Bussey TJ, Fawcett JW, Pizzorusso T, Saksida LM. **2013.** Depletion of perineuronal nets enhances memory and long-term depression in the perirhinal cortex. *Journal of Neuroscience* **33:** 7057-7065

Schulz DJ. **2006.** Plasticity and stability in neuronal output via changes in intrinsic excitability: it's what's inside that counts. *Journal of Experimental Biology* **209:** 4821-4827

Seeger G, Brauer K, Härtig W, Brückner G. **1994.** Mapping of perineuronal nets in the rat brain stained by colloidal iron hydroxide histochemistry and lectin cytochemistry. *Neuroscience* **58:** 371-388

Shah A, Lodge DJ. **2013.** A loss of hippocampal perineuronal nets produces deficits in dopamine system function: relevance to the positive symptoms of schizophrenia. *Nature Translational Psychiatry* **3:** e215

Slaker M, Barnes J, Sorg BA, Grimm JW. **2016.** Impact of environmental enrichment on perineuronal nets in the prefrontal cortex following early and late abstinence from sucrose self-administration in rats. *PLoS ONE* **11:** e0168256

Sorg BA, Berretta S, Blacktop JM, Fawcett JW, Kitagawa H, Kwok JCF, Miquel M. **2016.** Casting a wide net: role of perineuronal nets in neural plasticity. *Journal of Neuroscience* **36:** 11459-11468

Steullet P, Cabungcal JH, Bukhari SA, Ardelt MI, Pantazopoulos H, Hamati F, Salt TE, Cuenod M, Do KQ, Berretta S. **2017.** The thalamic reticular nucleus in schizophrenia and bipolar disorder: role of parvalbumin-expressing neuron networks and oxidative stress. *Molecular Psychiatry* **2017:** 1-9

Sugiyama S, Di Nardo AA, Aizawa S, Matsuo I, Volovitch M, Prochiantz A, Hensch TK. **2008.** Experience-dependent transfer of Otx2 homeoprotein into the visual cortex activates postnatal plasticity. *Cell* **134:** 508-520

Takesian AE, Hensch TK. **2013.** Balancing plasticity/stability across brain development. *Progress in Brain Research* **207:** 3-34

ten Donkelaar HJ, Bangma GC, de Boer-van Huizen R. **1985.** The fasciculus longitudinalis medialis in the lizard *Varanus exanthematicus*. *Anatomy and Embryology* **172:** 205-215

Thiele TR, Donovan JC, Baier H. **2014.** Descending control of swim posture by a midbrain nucleus in zebrafish. *Neuron* **83:** 679-691

Tsien R. **2013.** Very long-term memories may be stored in the pattern of holes in the perineuronal net. *Proceedings of the National Academy of Sciences* **110:** 12456-12461

Turrigiano GG. **2008.** The self-tuning neuron: synaptic scaling of excitatory synapses. *Cell* **135:** 422-435

Ueno H, Suemitsu S, Okamoto M, Matsumoto Y, Ishihara T. **2017.** Sensory experience-dependent formation of perineuronal nets and expression of CAT-315 immunoreactive components in the mouse somatosensory cortex. *Journal of Neuroscience* **355:** 161-174

Vo T, Carulli D, Ehlert EME, Kwok JCF, Dick G, Mecollari V, Moloney EB, Neufeld G, de Winter F, Fawcett JW, Verhaagen J. **2013.** The chemorepulsive axon guidance protein semaphorin3A is a constituent of perineuronal nets in the adult rodent brain. *Molecular and Cellular Neuroscience* **56:** 186-200

Wada N, Akenaga K, Takayama R, Tokuriki M. **1996.** Descending pathways from the medial longitudinal fasciculus and lateral vestibular nucleus to tail motoneurons in the decerebrate cat. *Archives Italiennes de Biologie* **134:** 207-215

Wang D, Ichiyama RM, Zhao R, Andrews MR, Fawcett. **2011.** Chondroitinase combined with rehabilitation promotes recovery of forelimb function in rats with chronic spinal cord injury. *Journal of Neuroscience* **31:** 9332-9344

Wegner F, Härtig W, Bringmann A, Grosche J, Wohlfarth K, Zuschratter W, Brückner G. **2003.** Diffuse perineuronal nets and modified pyramidal cells immunoreactive for glutamate and the $GABA_A$ receptor $\alpha 1$ subunit form a unique entity in rat cerebral cortex. *Experimental Neurology* **184:** 705-714

Yamada J, Jinno S. **2013.** Spatio-temporal differences in perineuronal net expression in the mouse hippocampus, with reference to parvalbumin. *Journal of Neuroscience* **253:** 368-379

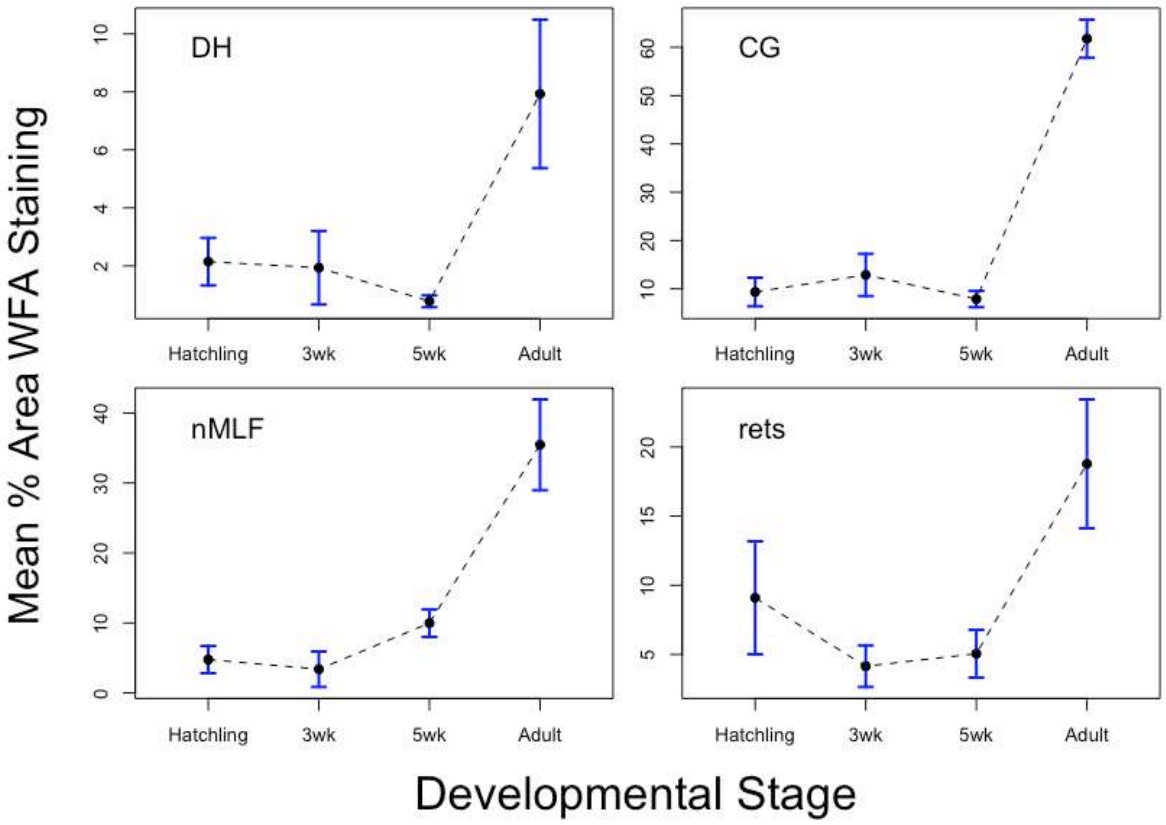

Figure A1.1. PNN trajectories for all regions in *Poecilia reticulata.* Means ± SEM. This figure is identical to Figure 3.3A, but is placed here for convenient comparison with other species.

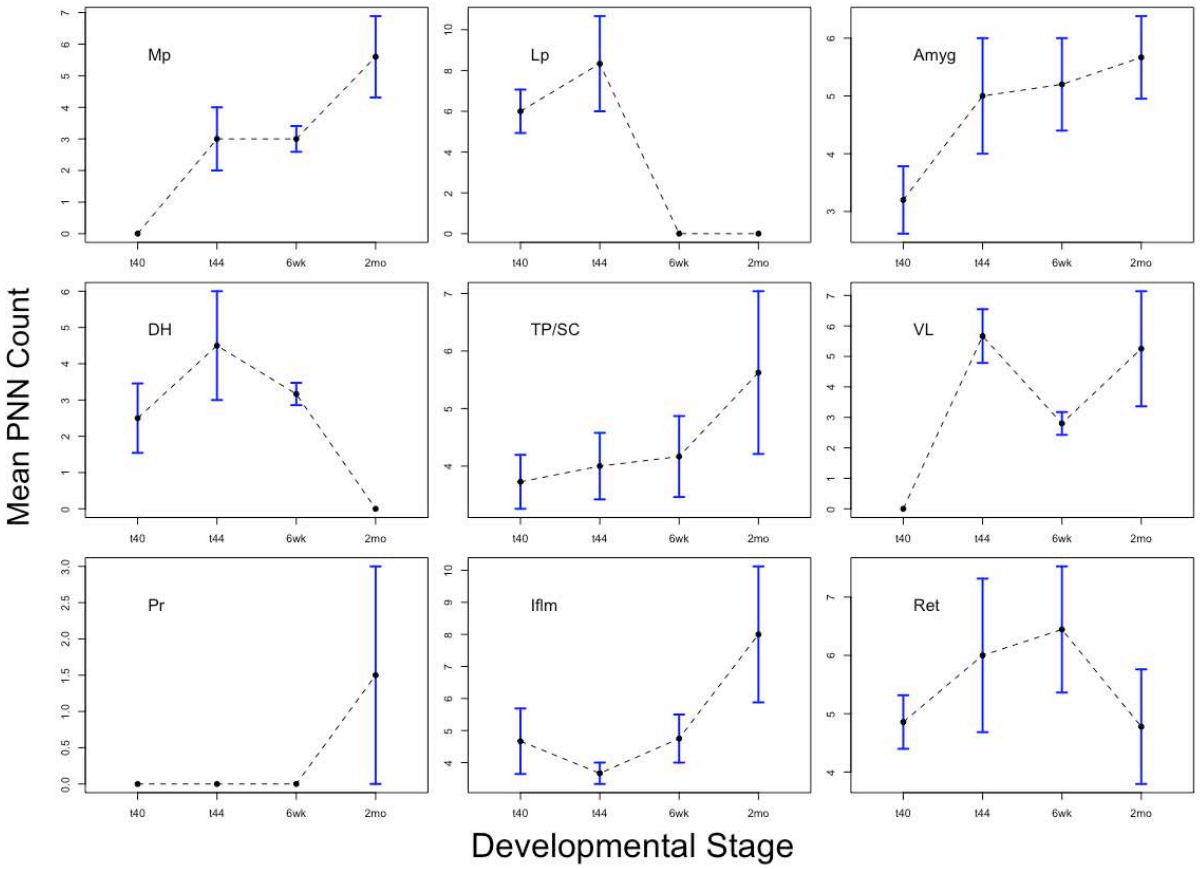

Figure A1.2. PNN trajectories for all regions in *Rhinella yunga.* Means ± SEM. See Table 1.1 for list of abbreviations for region names.

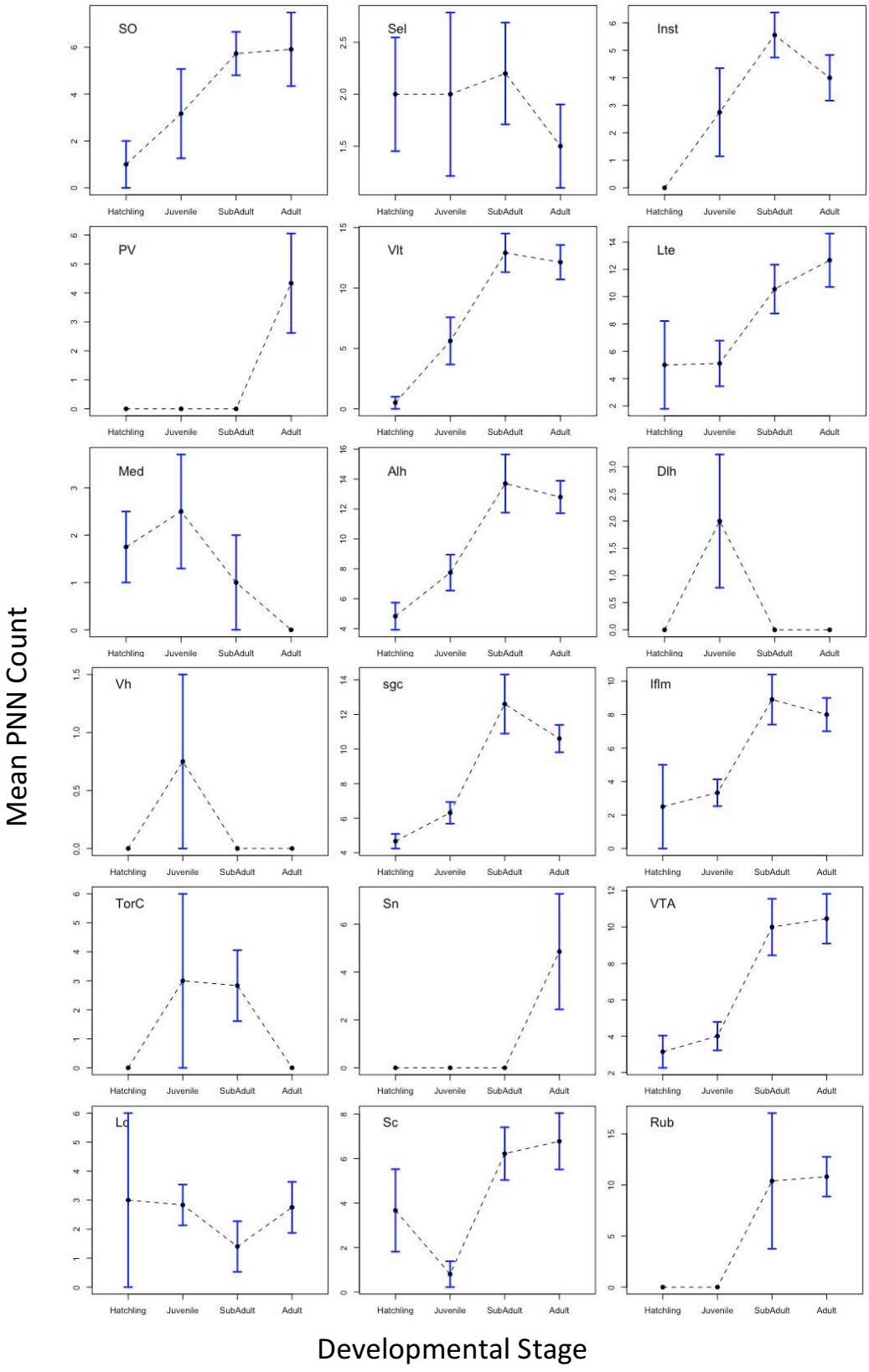

Figure A1.3. PNN trajectories for all regions in *Anolis sagrei.* Means ± SEM. See Table 1.1 for list of abbreviations for region names.

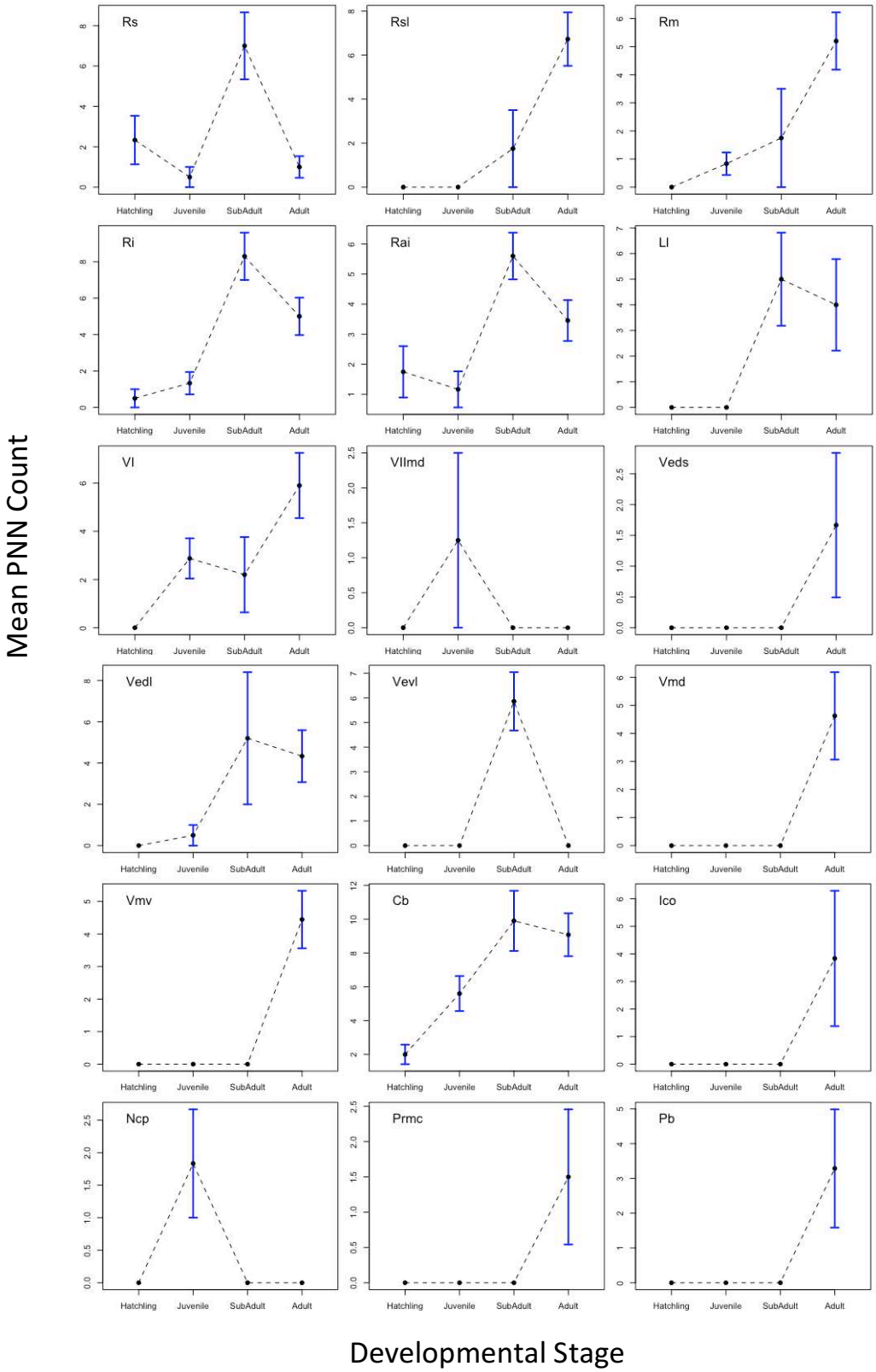

Figure A1.3. Continued from previous page.